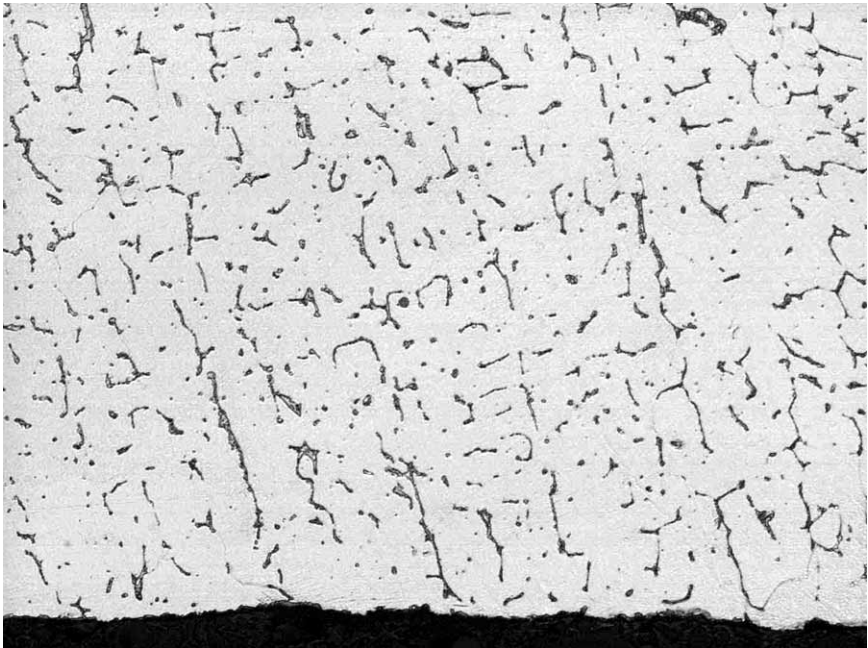
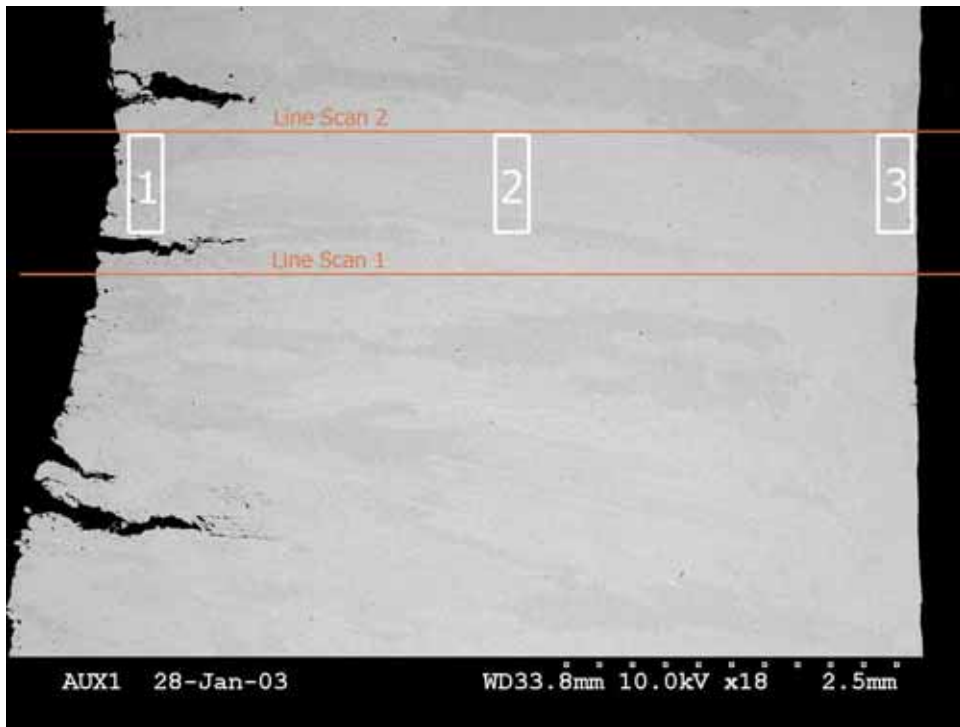


100X

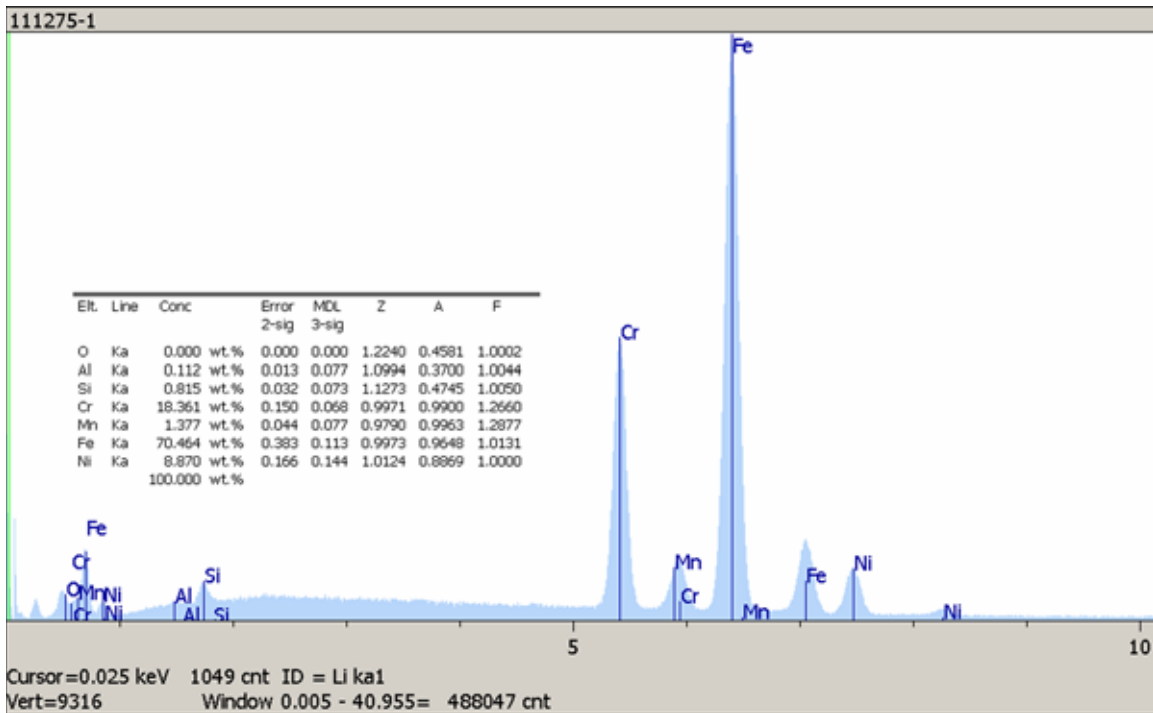


375X

Figure 6.1.1.5: Typical clad microstructure near RCS side surface of the cladding. No intergranular attack (IGA) was present.

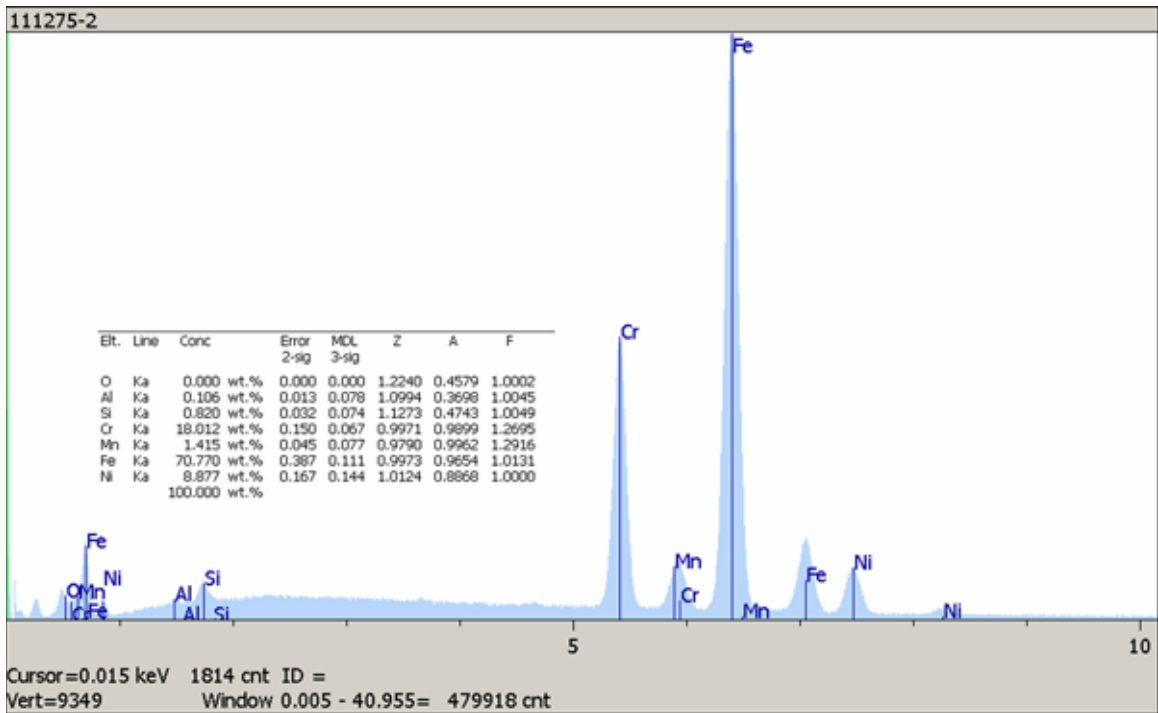


SEM micrograph showing EDS locations.

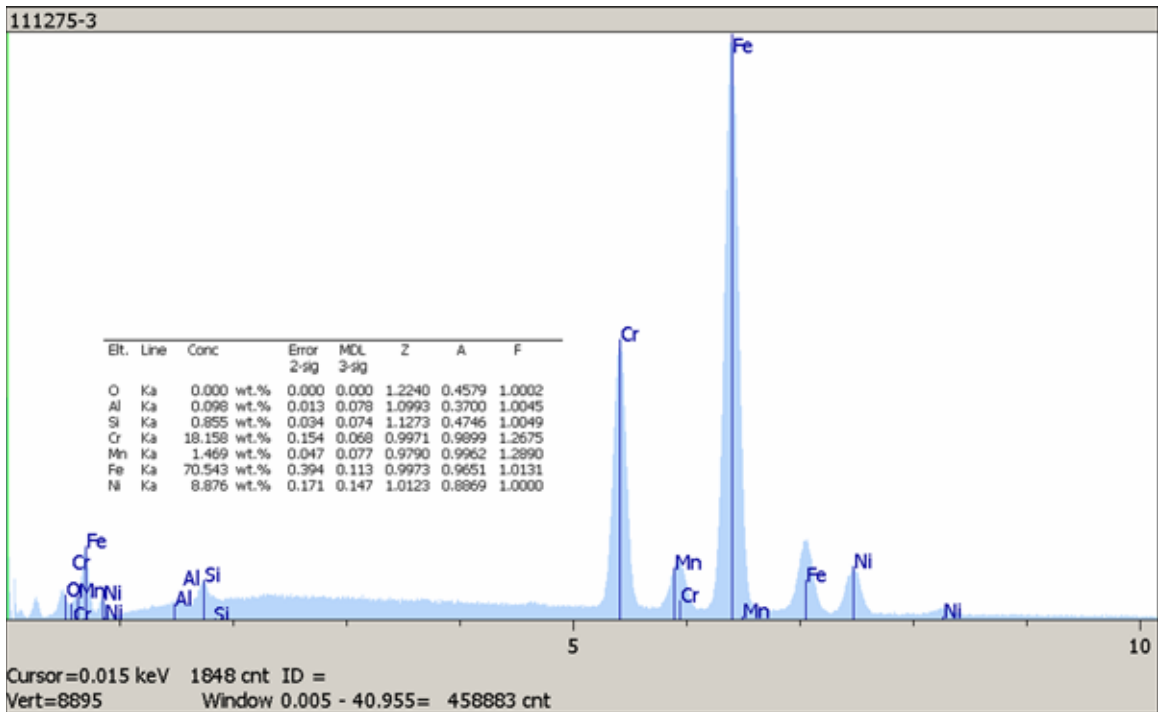


EDS results for Area 1.

Figure 6.1.2.1: SEM micrograph showing the three deepest cracks in A2A7M. Crack tips are 0.042" to 0.069" (1.1 to 1.75 mm) below the surface. It is noted that these three crack tips are at approximately the same distance of 0.199" (5.06 mm) from the underside surface. EDS scans of areas 1, 2, and 3 and line scans 1 and 2 (not included) indicated a generally uniform chemical composition (including Cr content) across the cladding thickness.

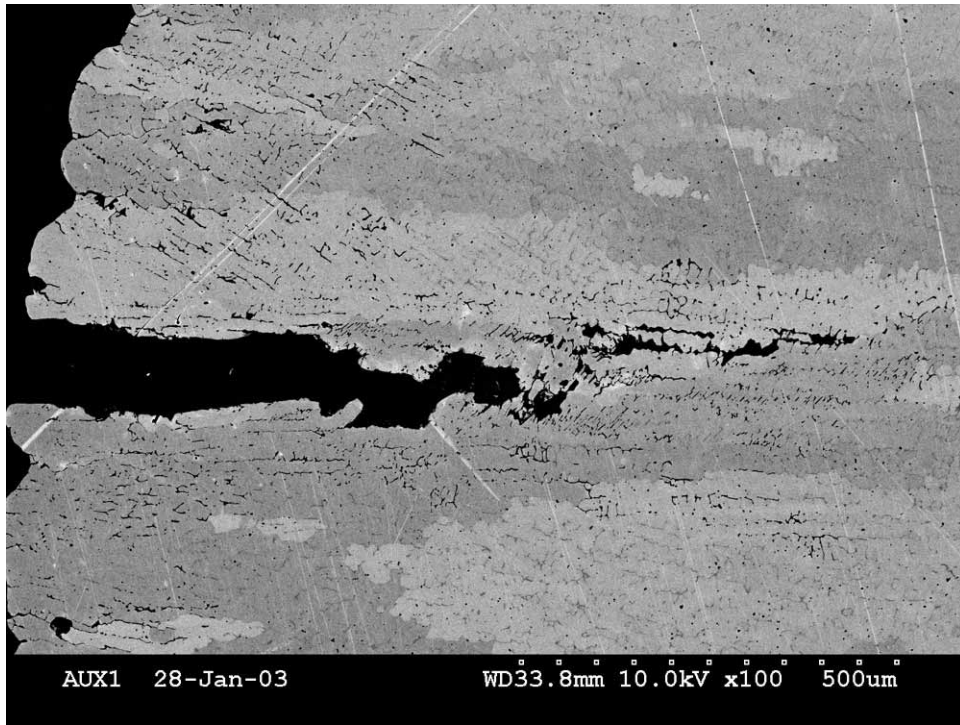


EDS results for Area 2.

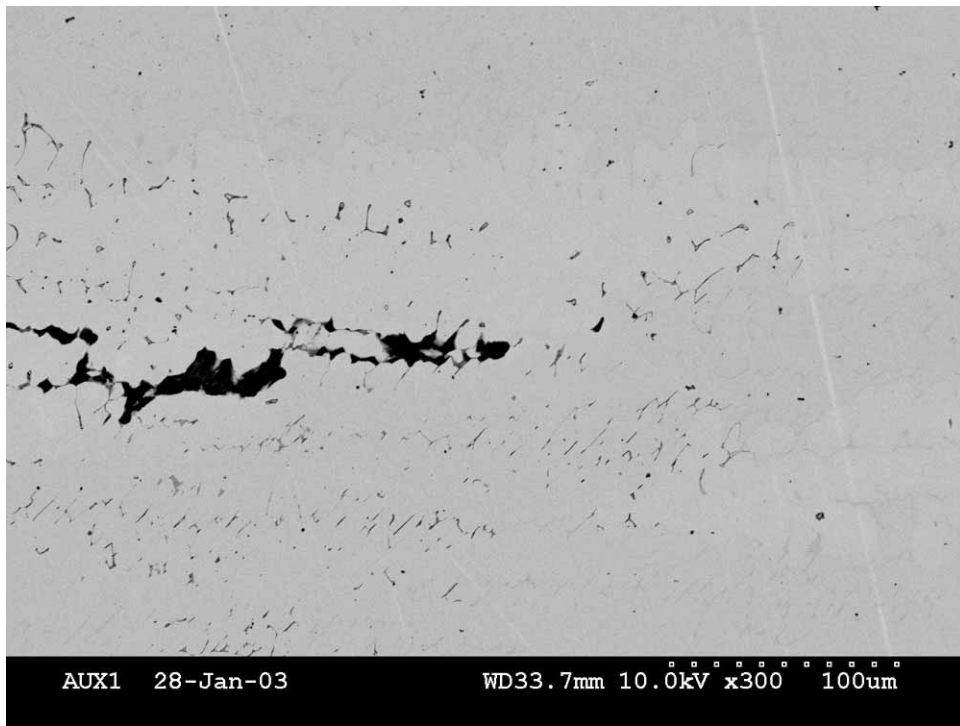


EDS results for Area 3.

Figure 6.1.2.1 (cont.): EDS results for Areas 2 and 3.



100X



300X

Figure 6.1.2.2: SEM micrographs showing interdendritic crack path along the elongated ferrite pools.

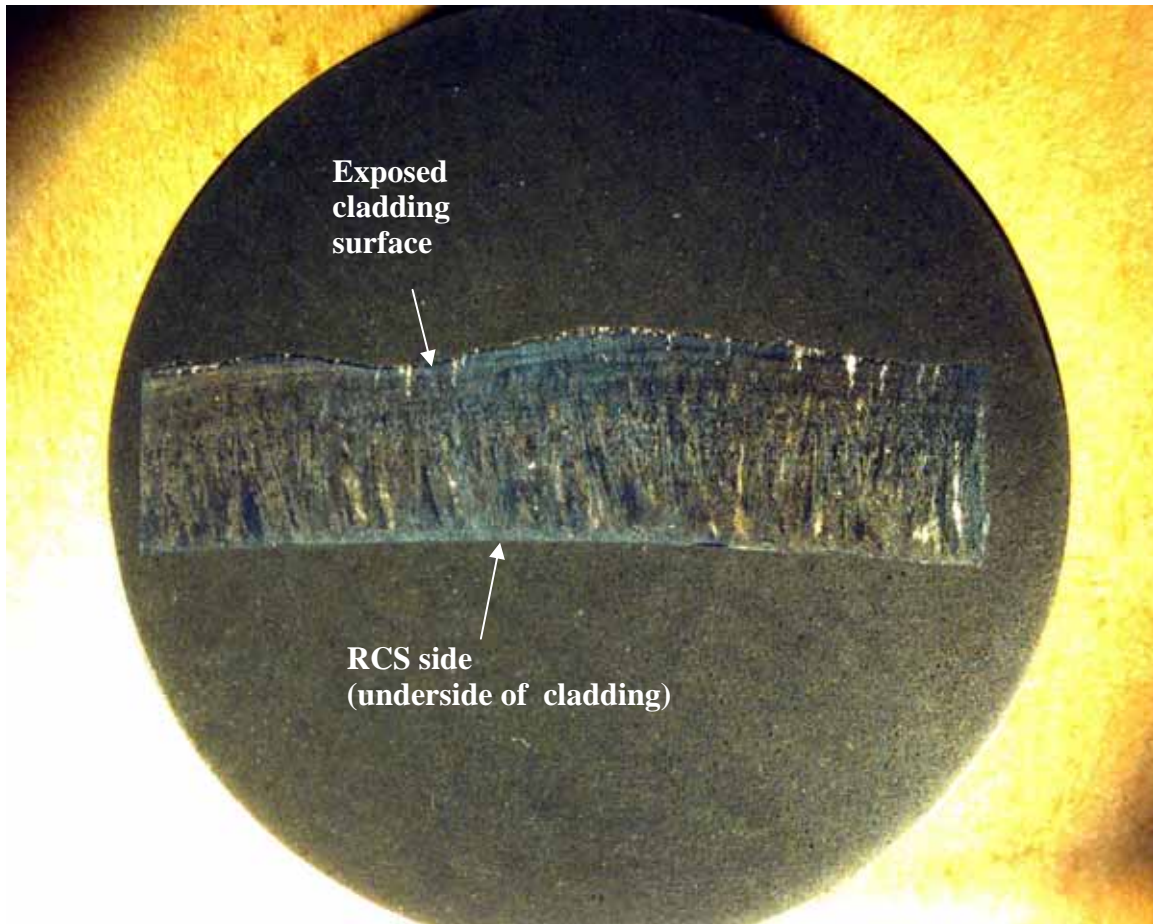
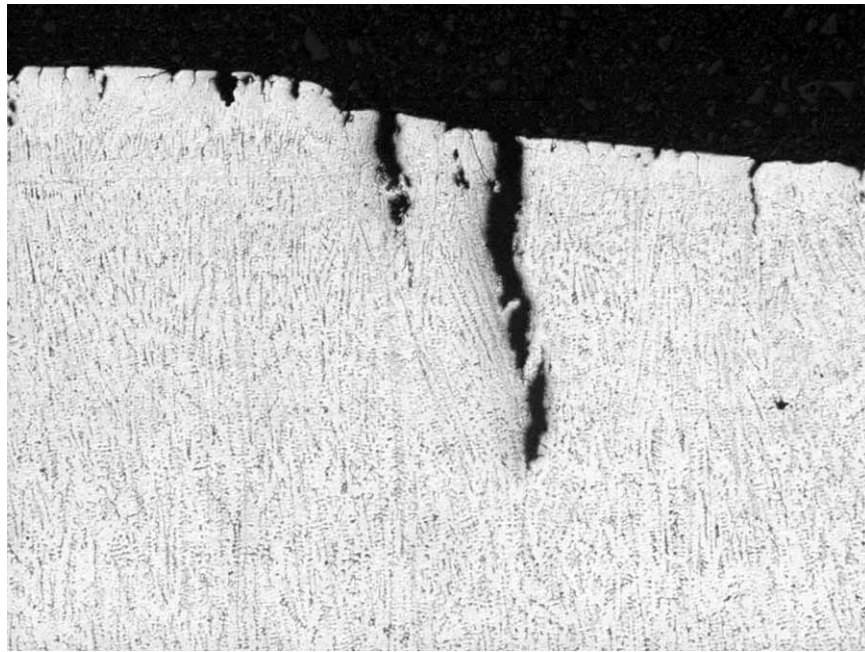
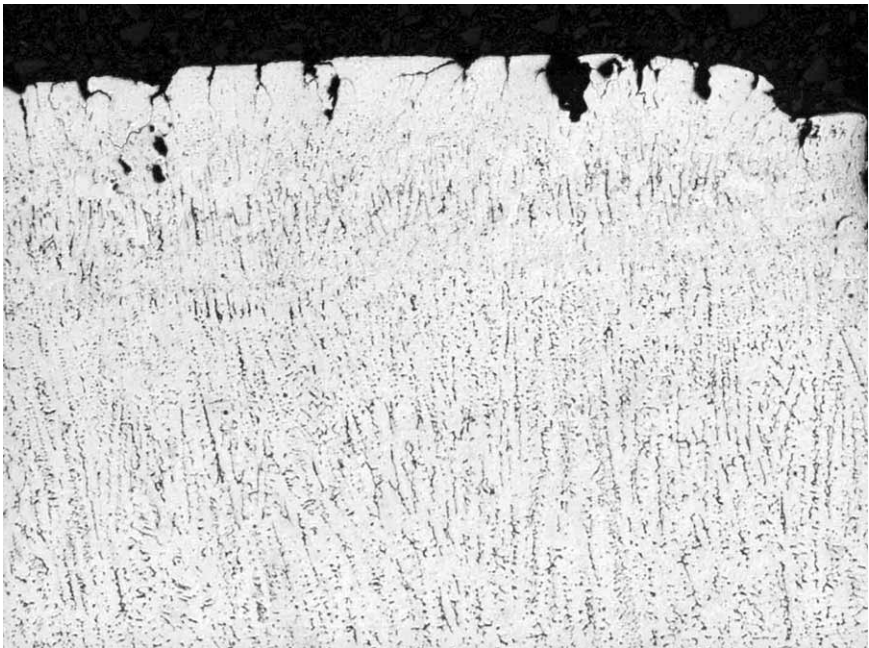


Figure 6.2.1.1: 4X macro photograph of metallurgical mount A2A7N. Refer to Figure 5.11 for the sample orientation.

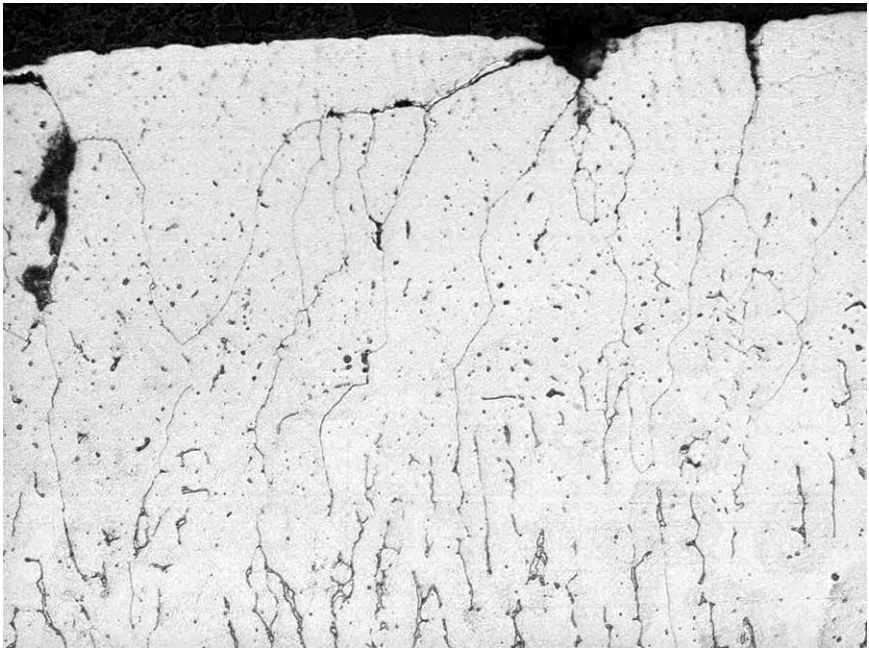


Etched 48X

Figure 6.2.1.2: Micrograph of a crack observed on A2A7N. The crack tip is estimated to be approximately 0.036" (0.91 mm) below the surface.

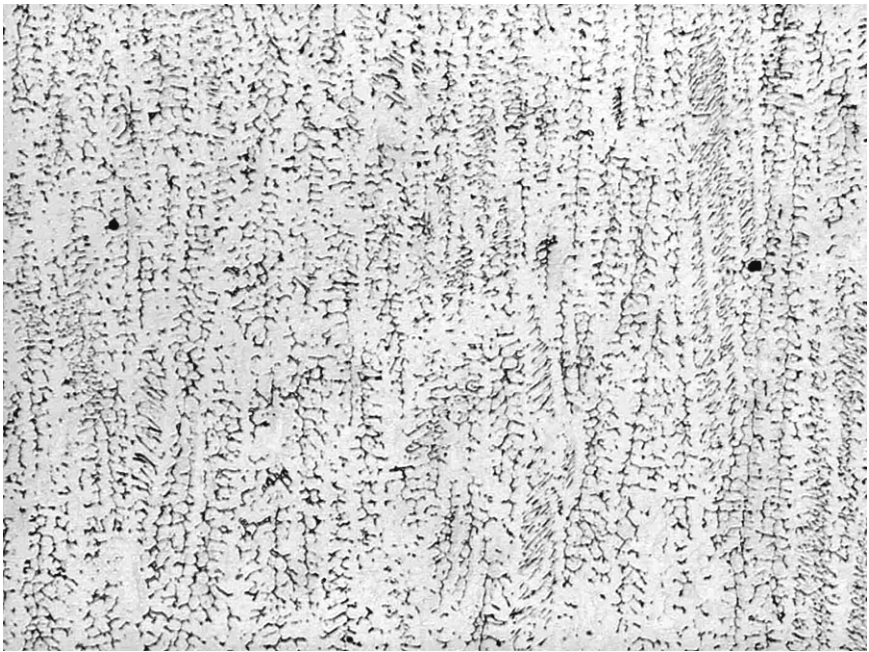


100X

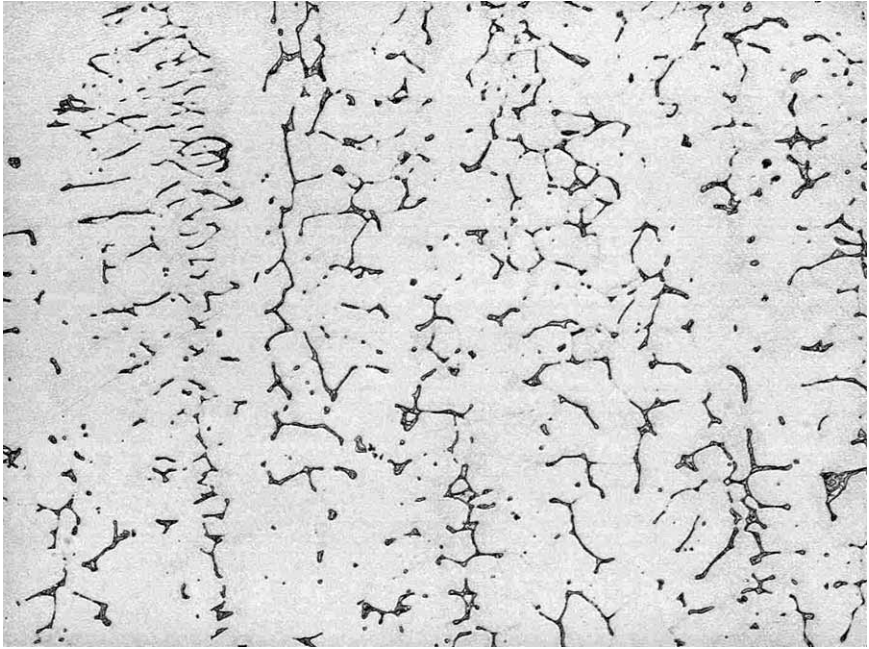


375X

Figure 6.2.1.3: Micrographs showing intergranular attack (IGA) and intergranular cracking on the exposed stainless steel cladding.

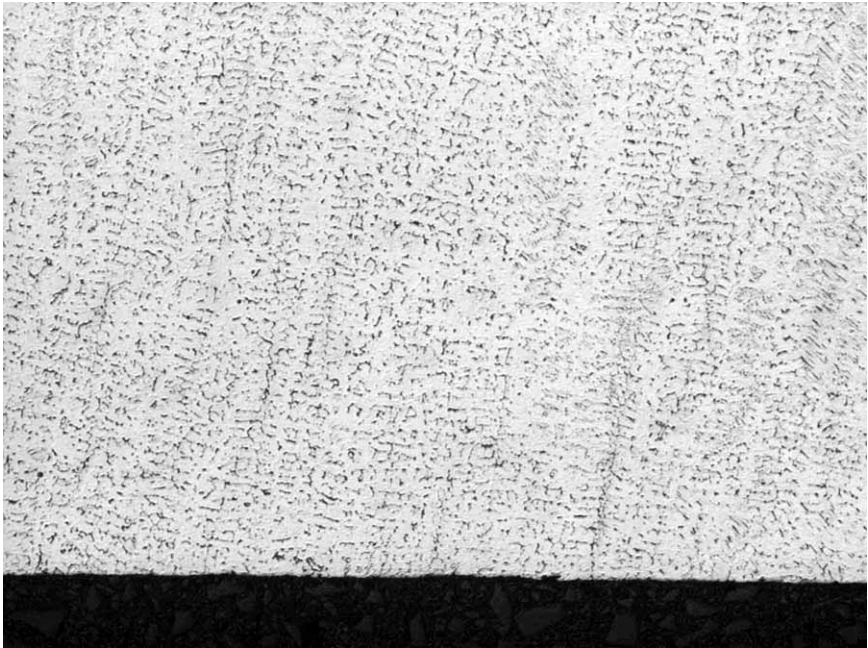


100X

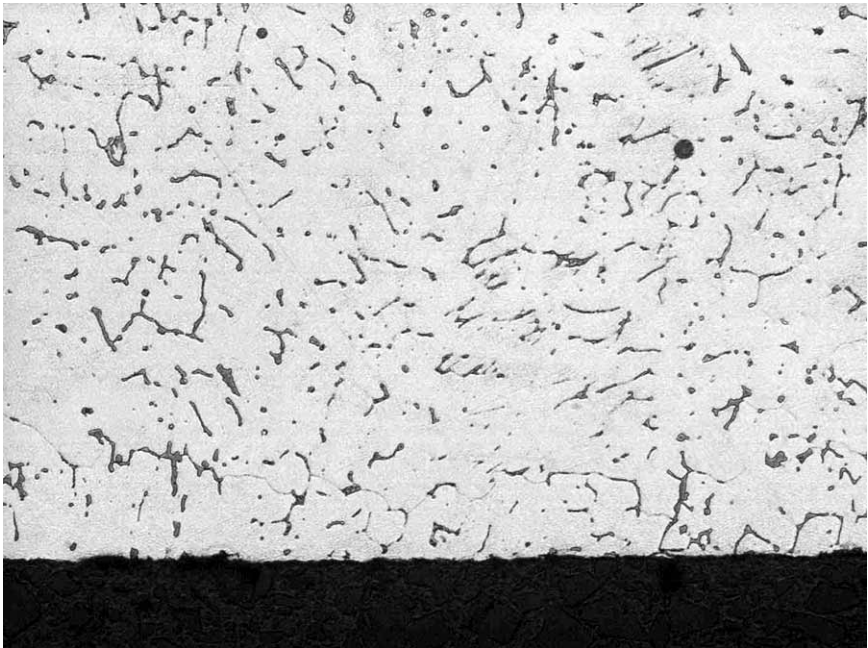


375X

Figure 6.2.1.4: Typical clad microstructure in the mid-thickness of the cladding.

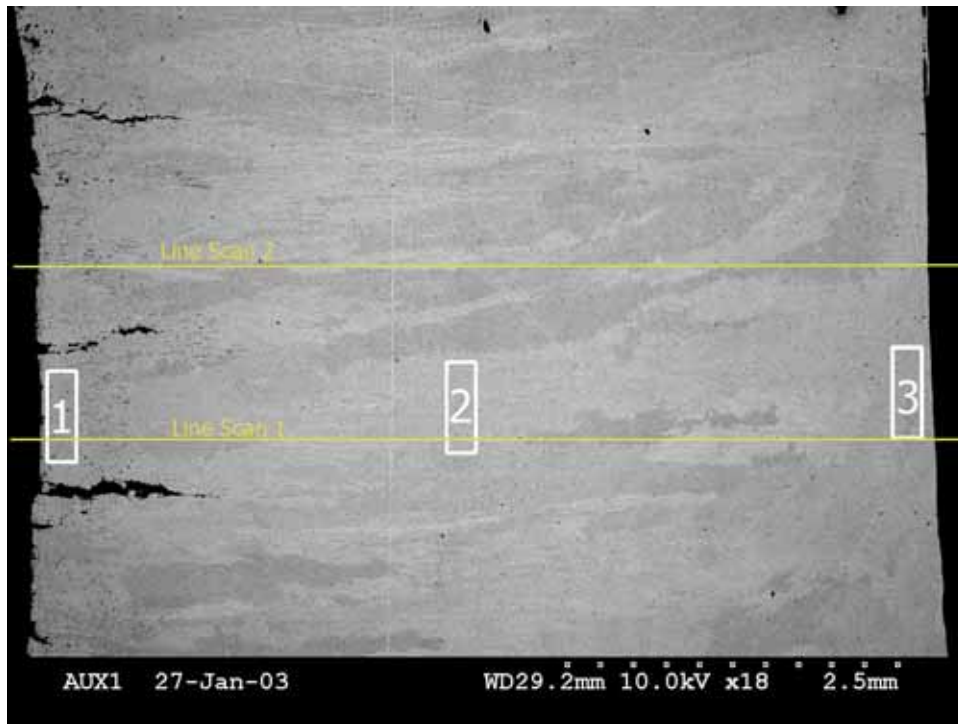


100X

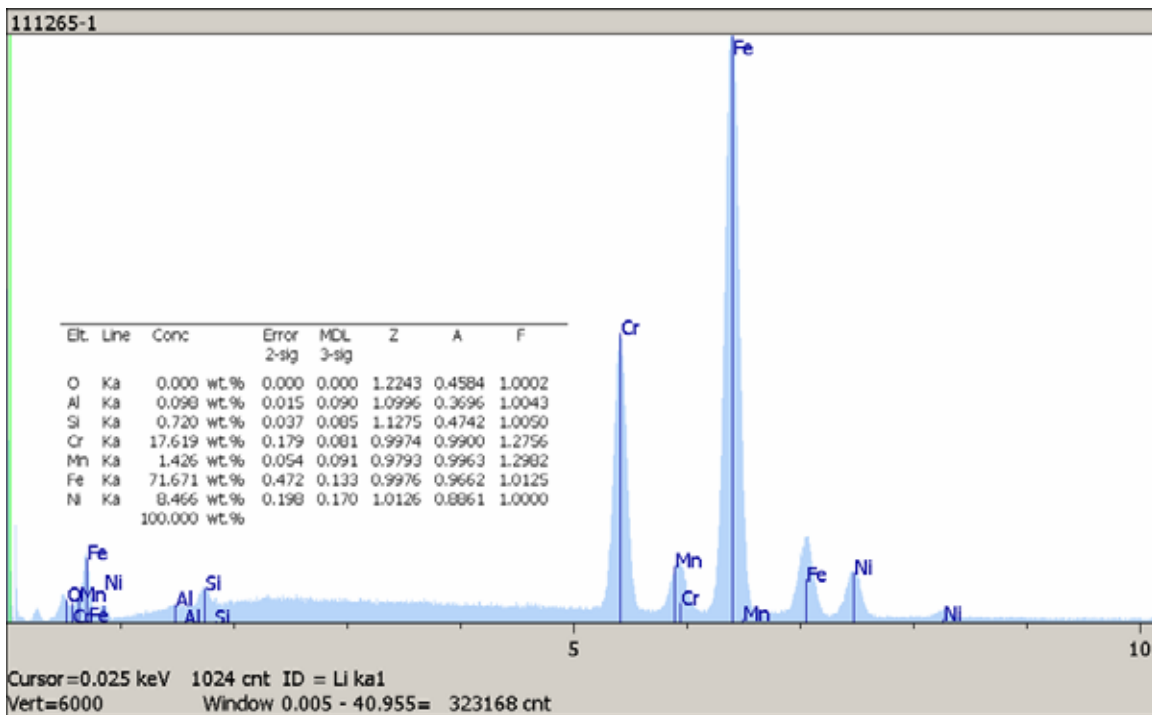


375X

Figure 6.2.1.5: Typical clad microstructure near RCS side surface of the cladding. No intergranular attack (IGA) was present.

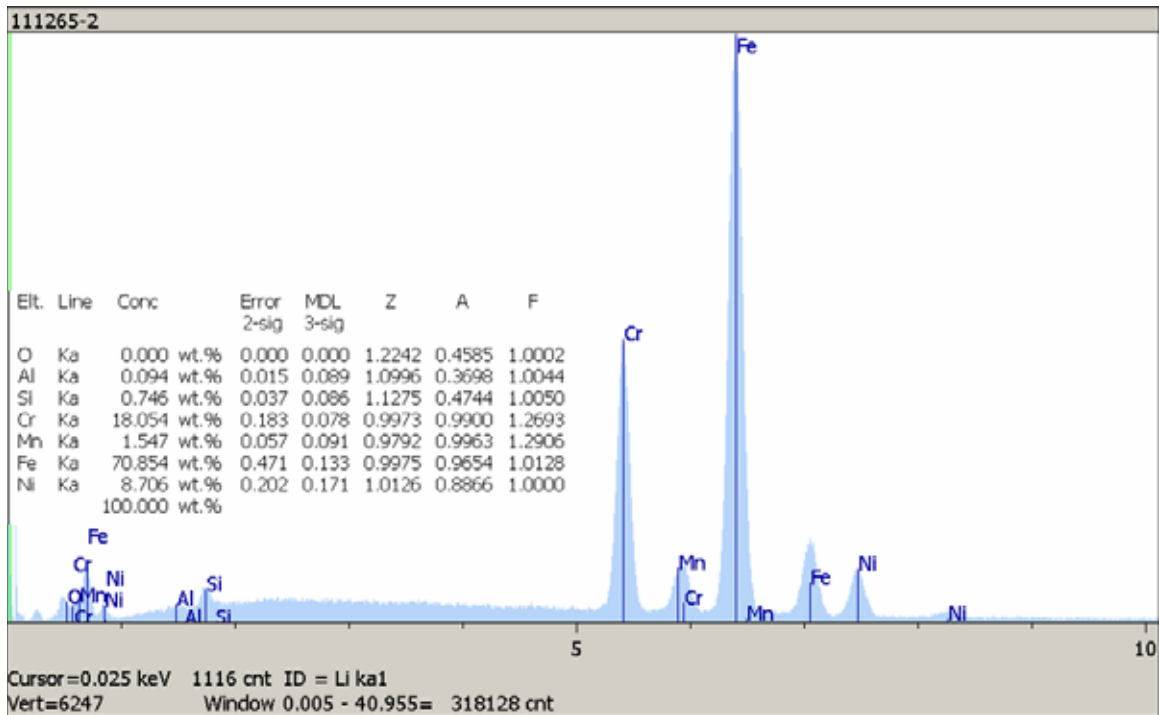


SEM micrograph showing EDS locations.

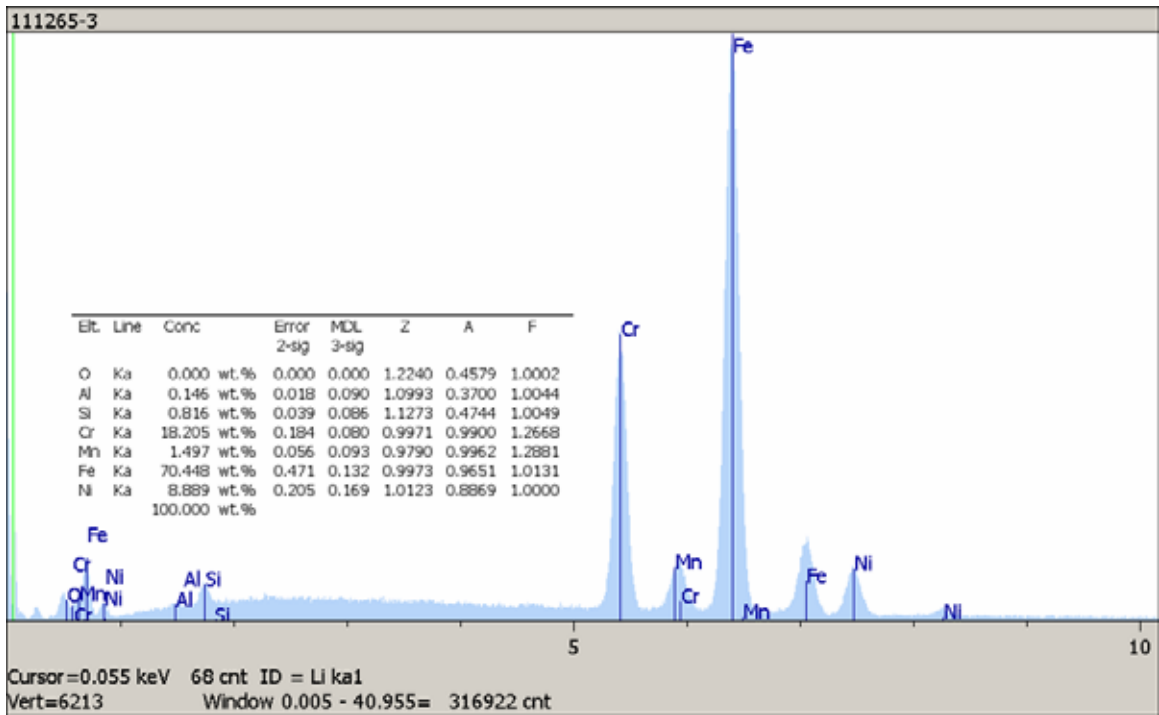


EDS results for Area 1.

Figure 6.2.2.1: SEM micrograph showing the three deepest cracks in A2A7N. The maximum crack depth was approximately 0.056" (1.42 mm). EDS scans of areas 1, 2, and 3 and lines 1 and 2 (not included) indicated a generally uniform chemical composition (including Cr content) across the cladding thickness.

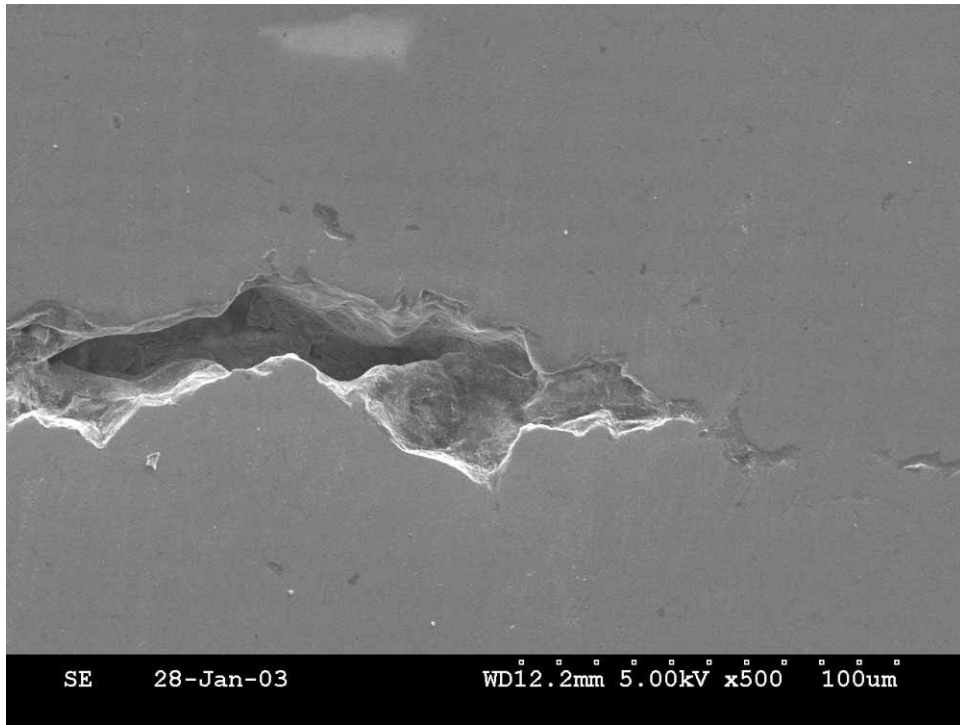


EDS results for Area 2.

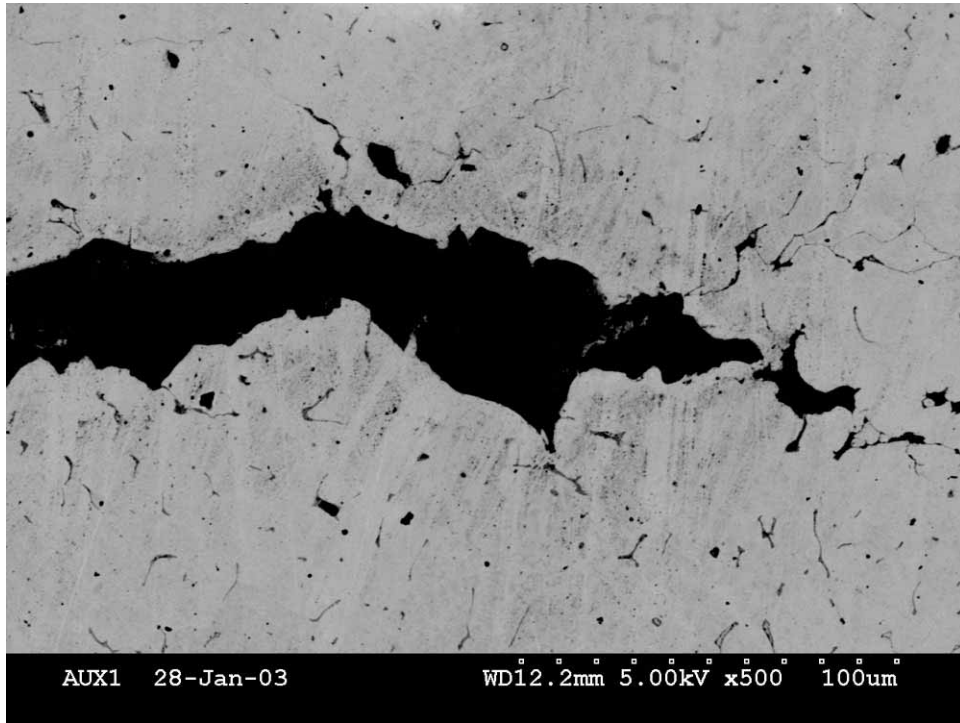


EDS results for Area 3.

Figure 6.2.2.1 (cont.): EDS results for Areas 2 and 3.



SE 500X



BSE 500X

Figure 6.2.2.2: Higher magnification SEM micrographs of crack tip, showing the interdendritic crack path along the elongated ferrite pools.

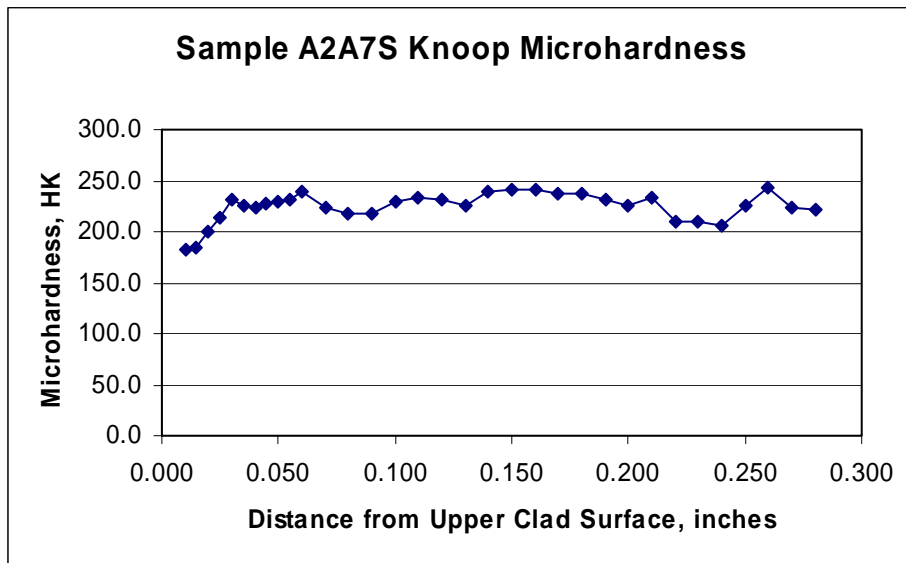
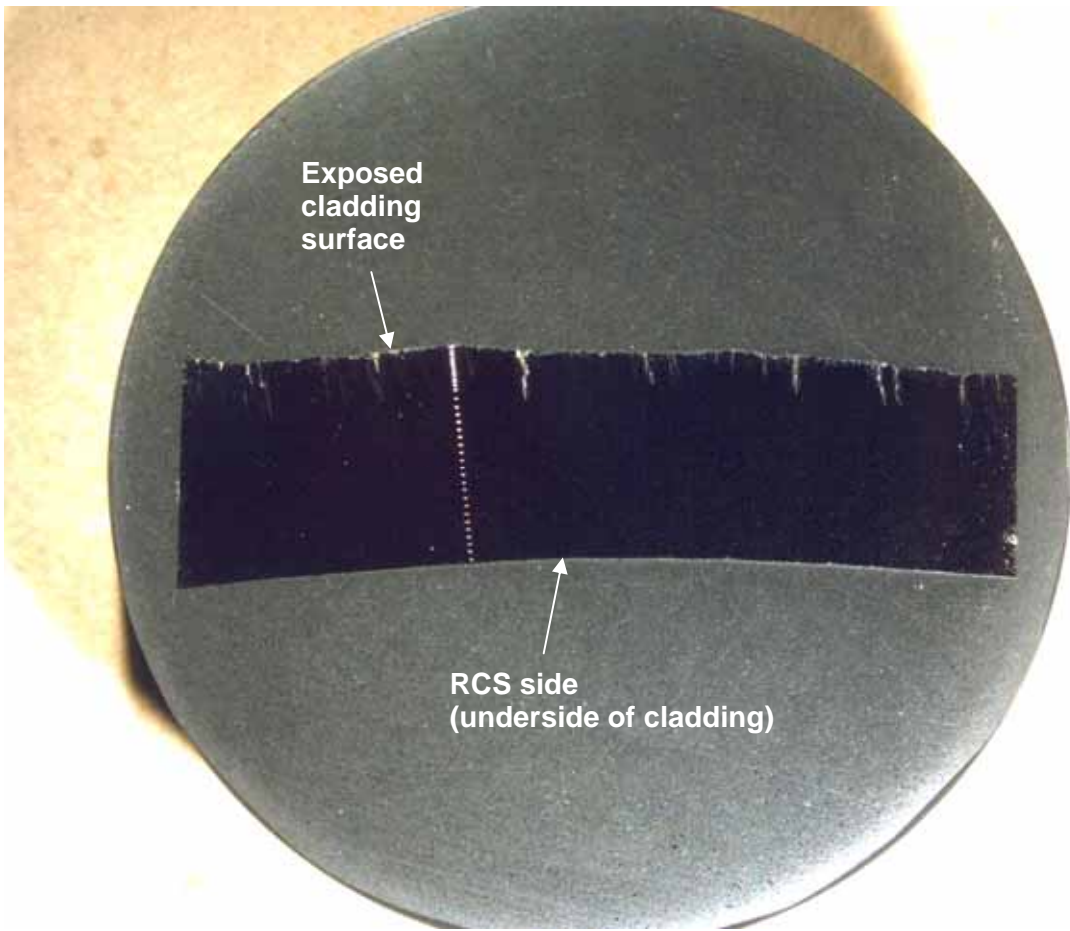
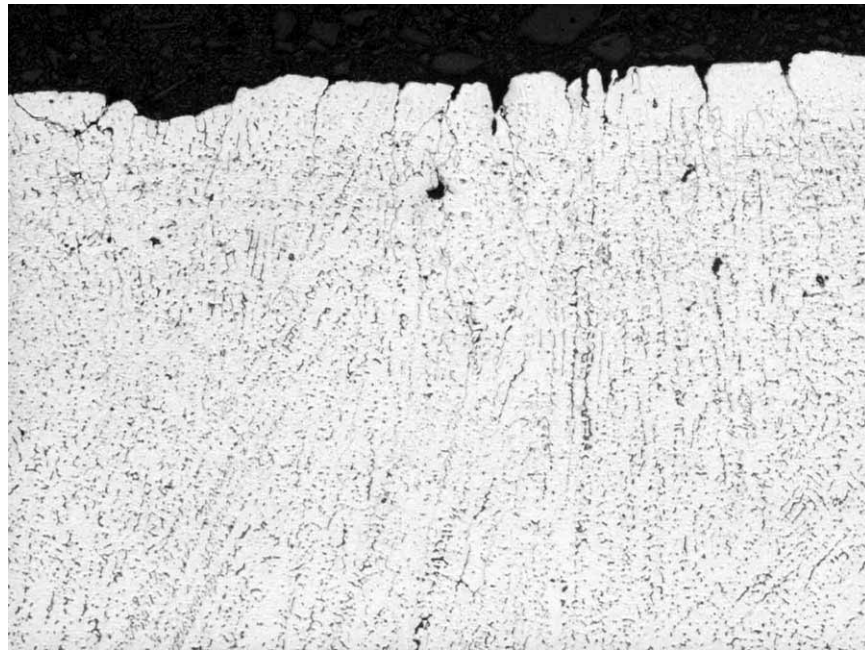
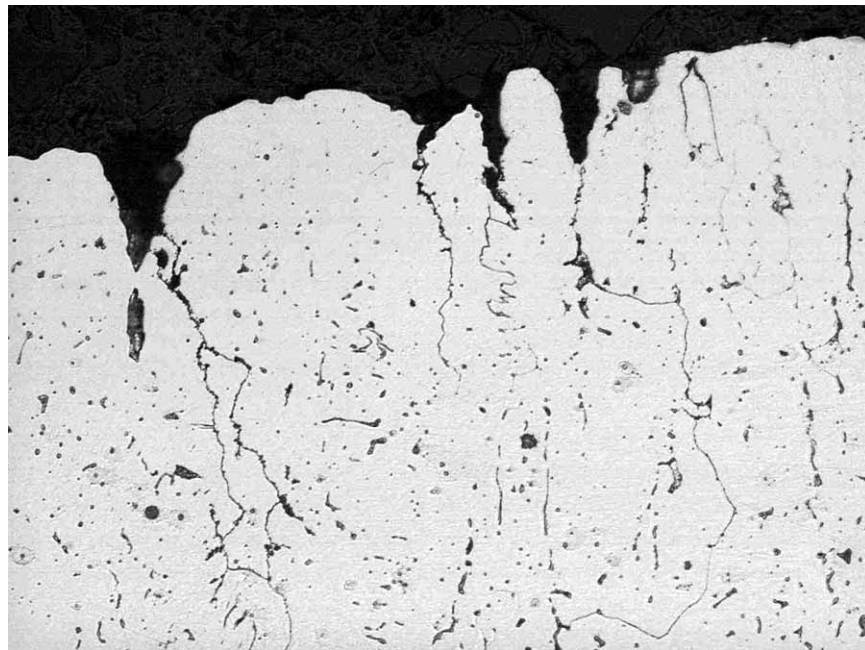


Figure 6.3.1.1: 4X macro photograph of metallurgical mount A2A7S. Refer to Figure 5.11 for the sample orientation. Knoop microhardness values exhibited lower hardness readings toward the exposed clad side (left side of graph), which was in contrast to A2A7M.

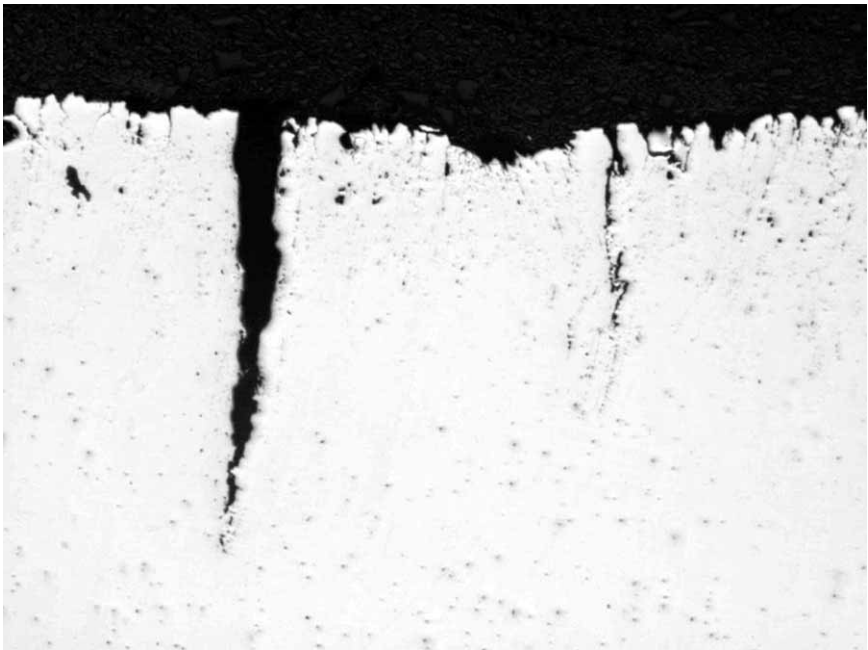


100X

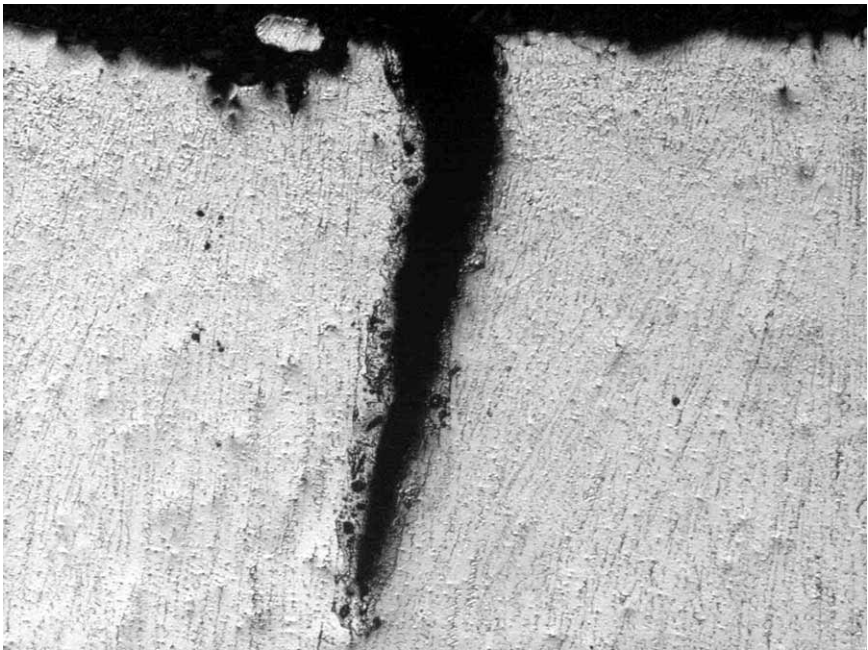


375X

Figure 6.3.1.2: Micrographs showing intergranular attack (IGA) and intergranular or interdendritic cracking on the exposed stainless steel cladding.

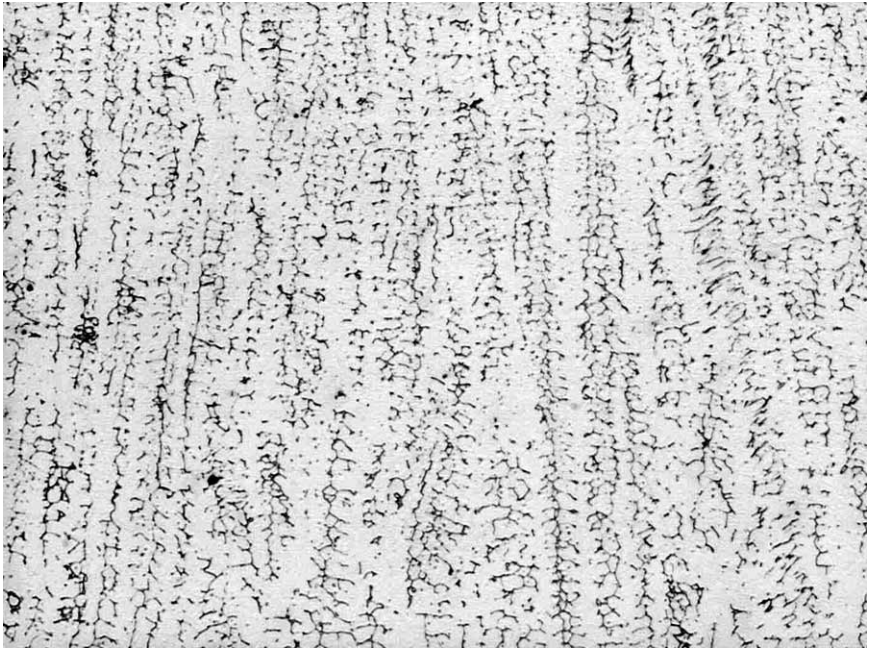


As-polished 48X

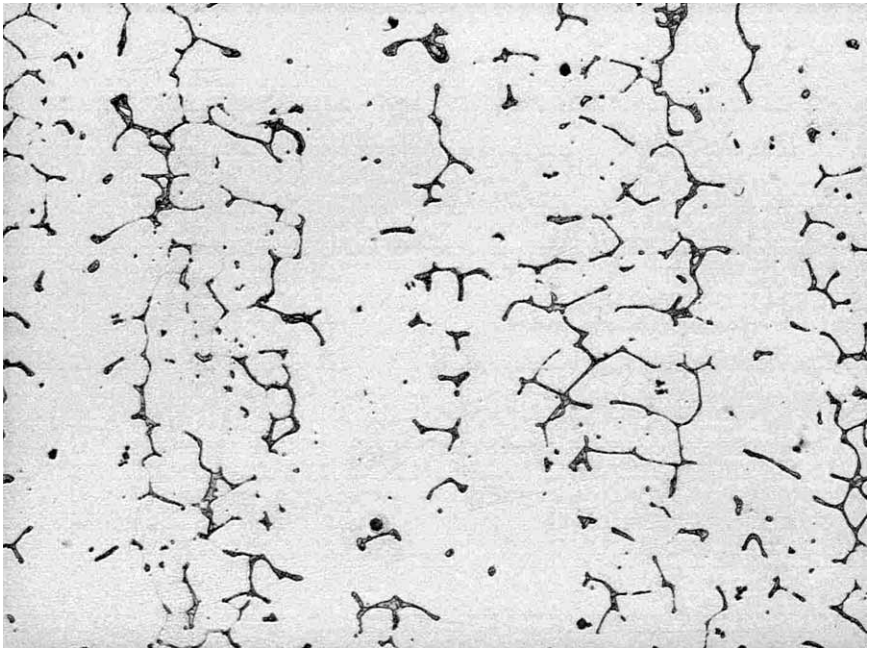


Etched 48X

Figure 6.3.1.3: Micrographs of cracking observed on sample A2A7S. Different cracks are shown.

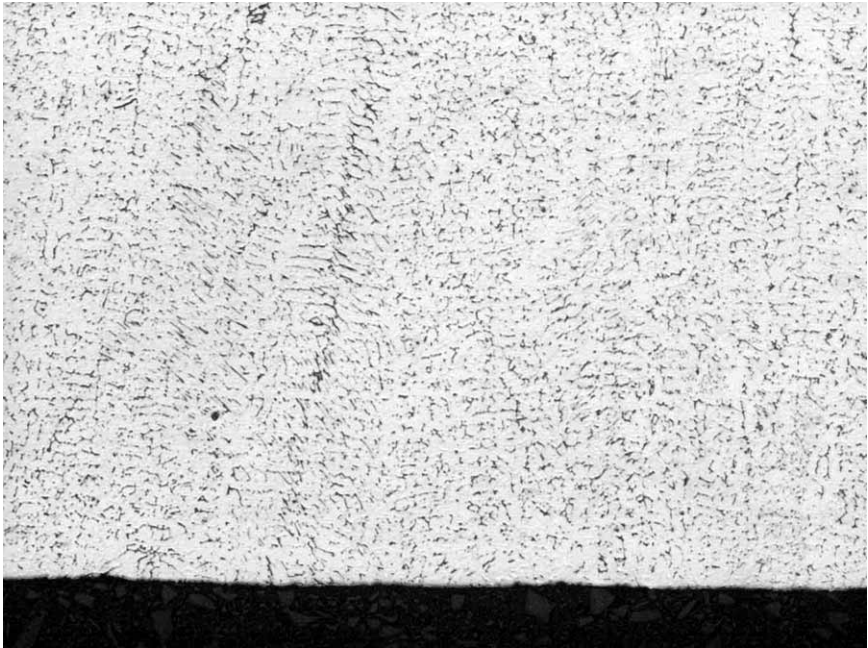


100X

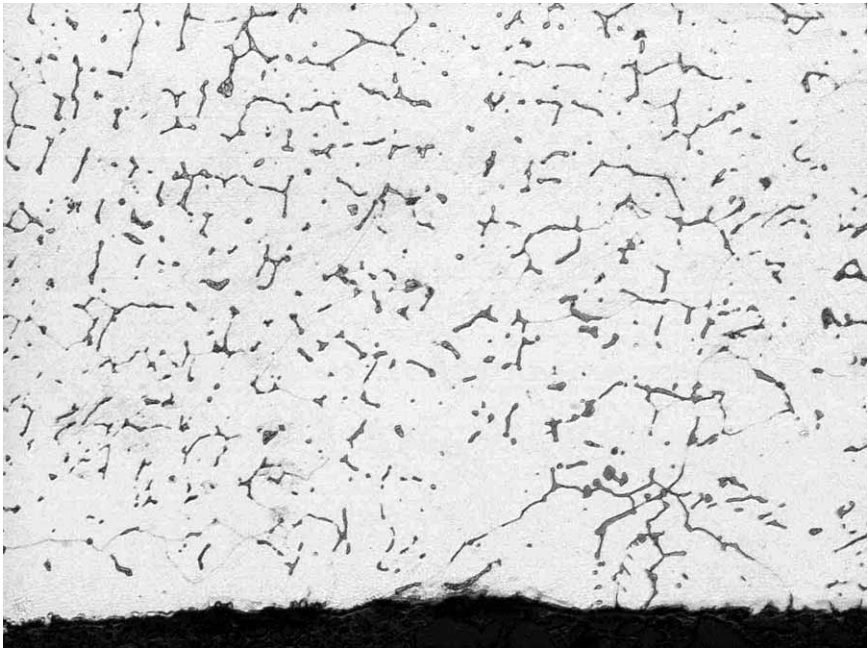


375X

Figure 6.3.1.4: Typical clad microstructure in the mid-thickness of the cladding.

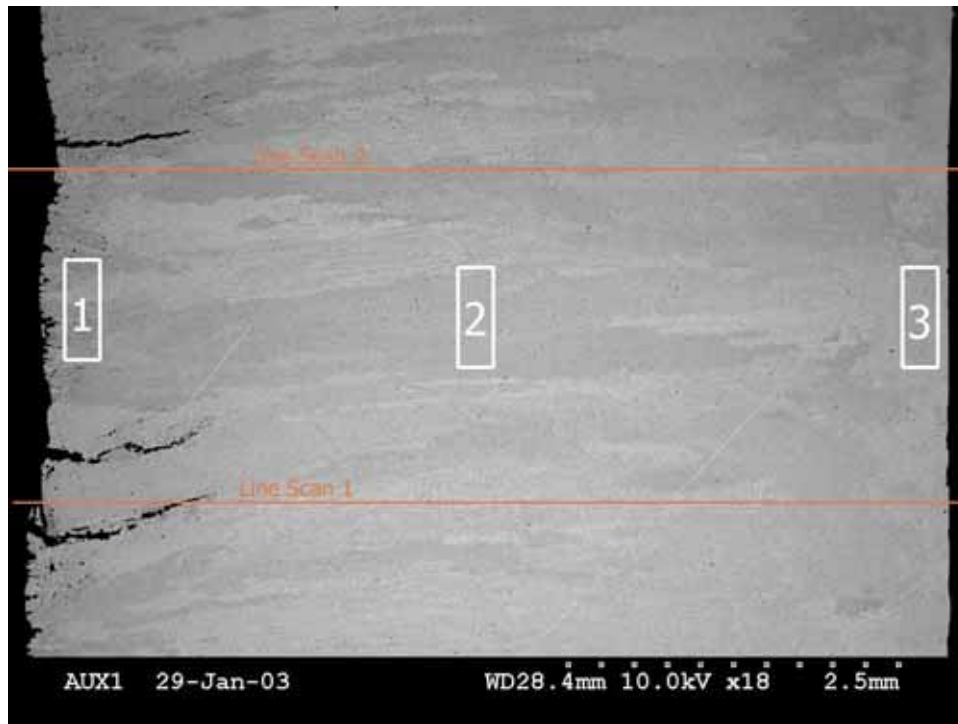


100X

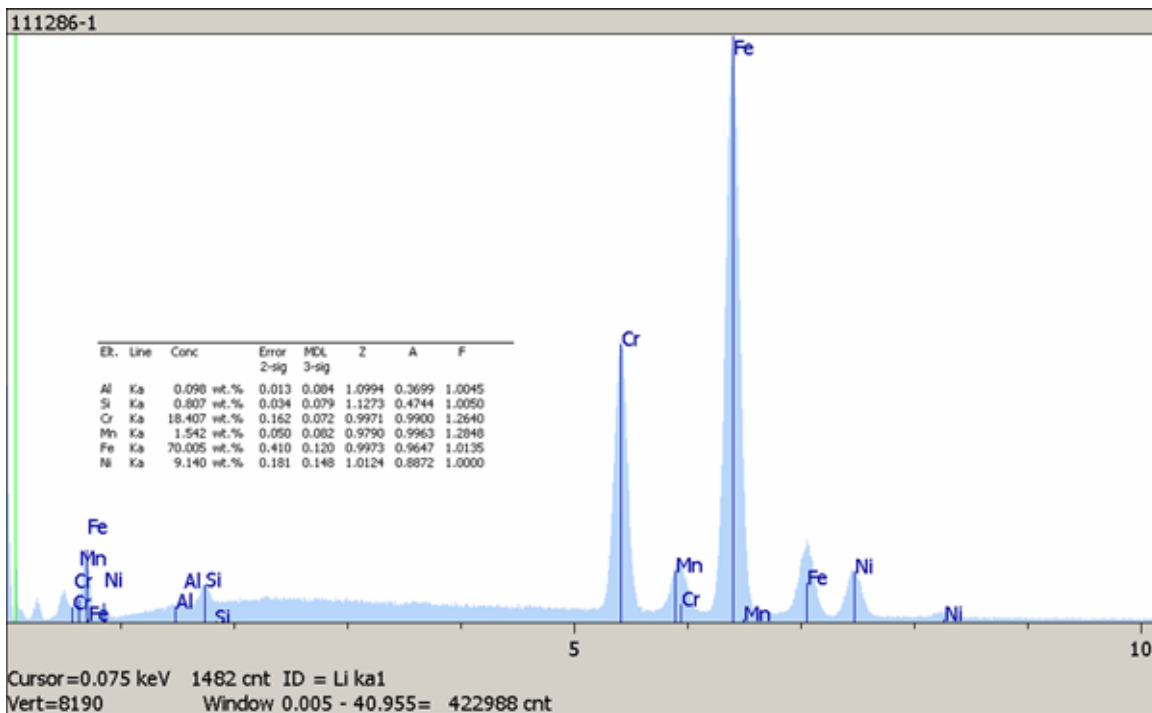


375X

Figure 6.3.1.5: Typical clad microstructure near RCS side surface of the cladding. No intergranular attack (IGA) was present.

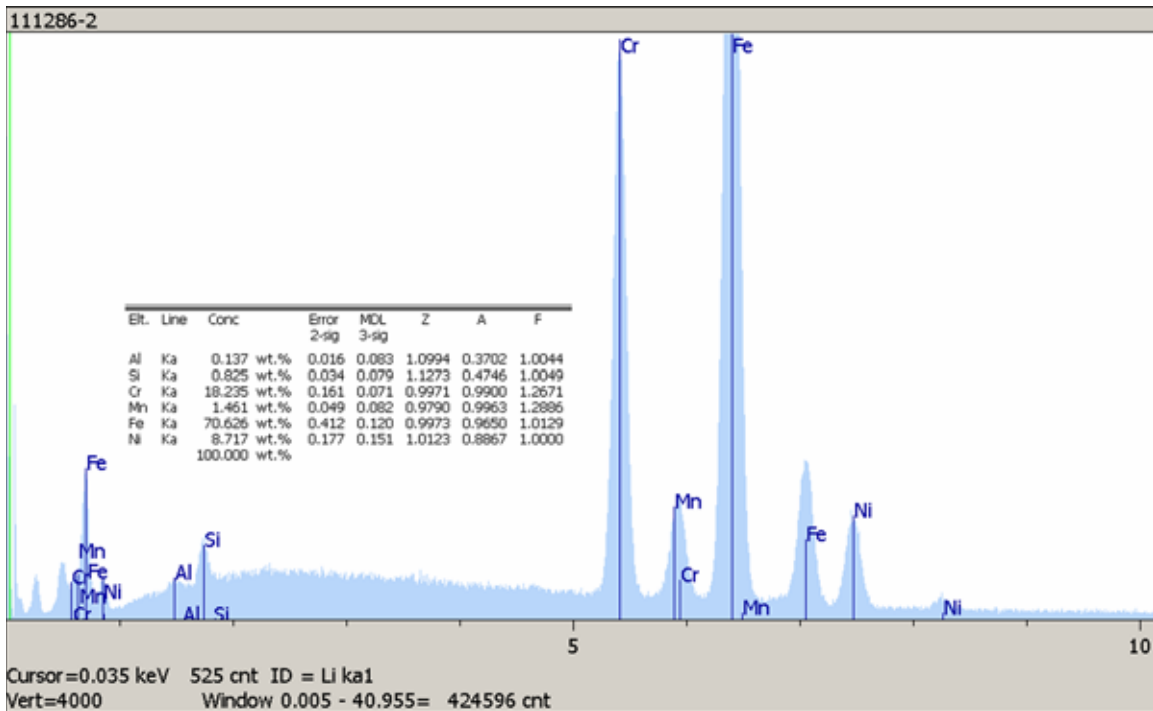


SEM micrograph showing EDS locations.

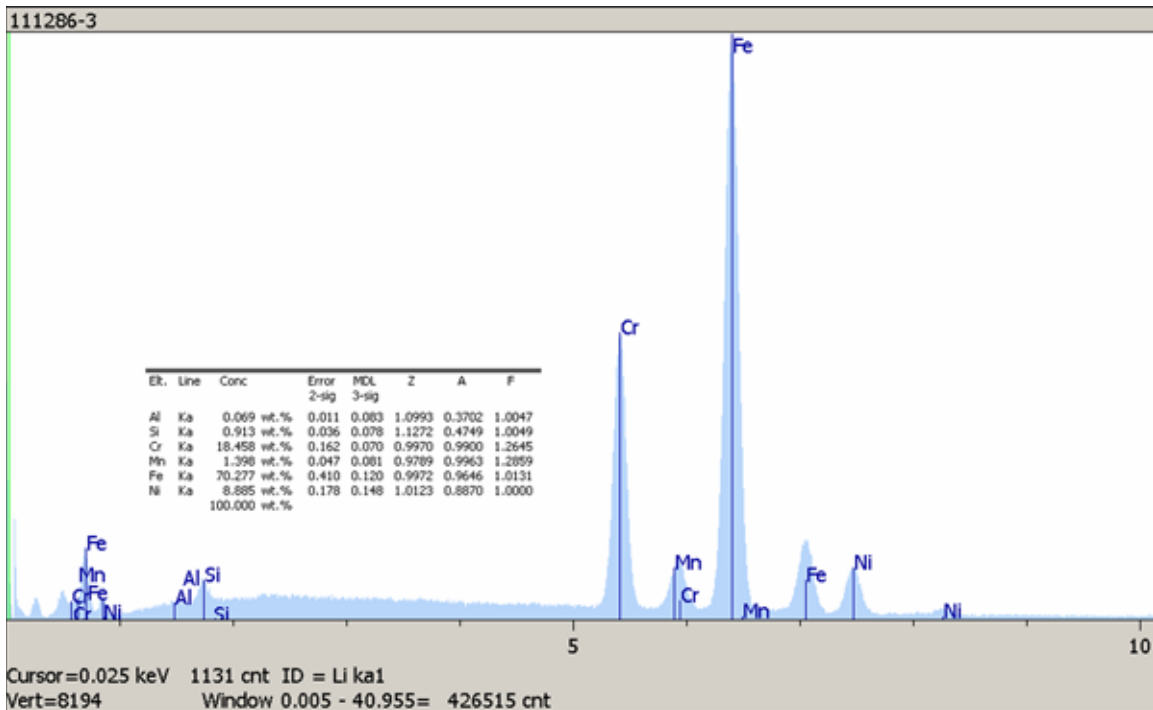


EDS results for Area 1.

Figure 6.3.2.1: SEM micrograph of the three deepest cracks in A2A7S. The maximum crack depth was approximately 0.056" (1.42 mm). These three crack tips are approximately the same distance from the underside surface. EDS scans of areas 1, 2, and 3 and lines 1 and 2 (not included) indicated a generally uniform chemical composition (including Cr content) across the cladding thickness.



EDS results for Area 2.



EDS results for Area 3.

Figure 6.3.2.1 (cont.): EDS results for Areas 2 and 3. Note that the Cr peak was set at full screen height for Area 2.

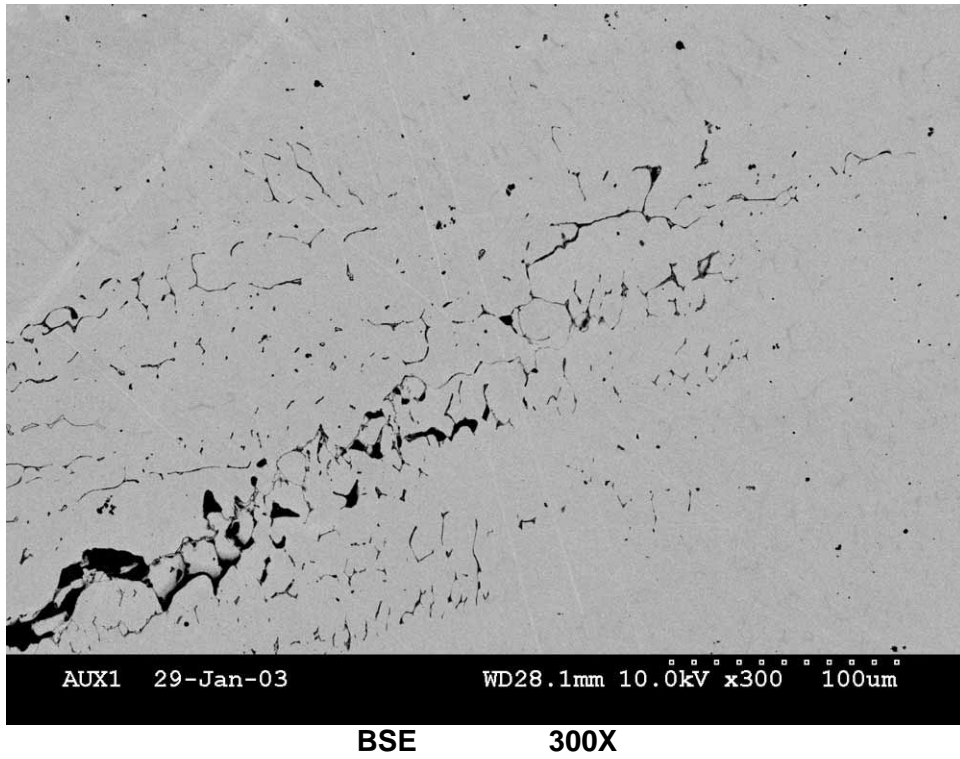
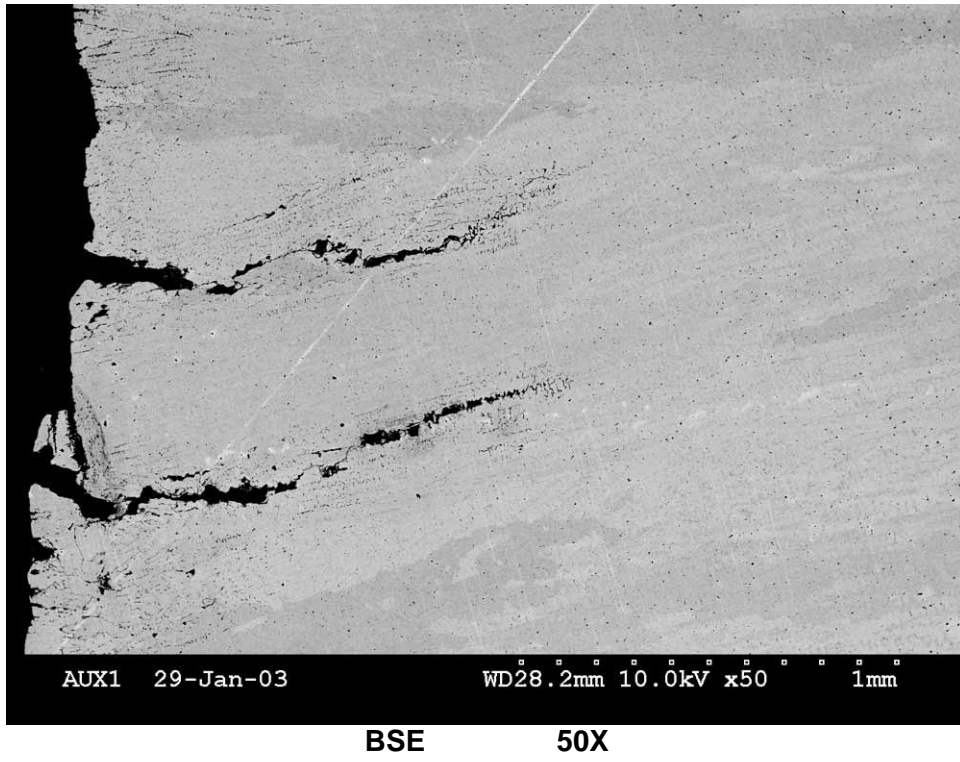
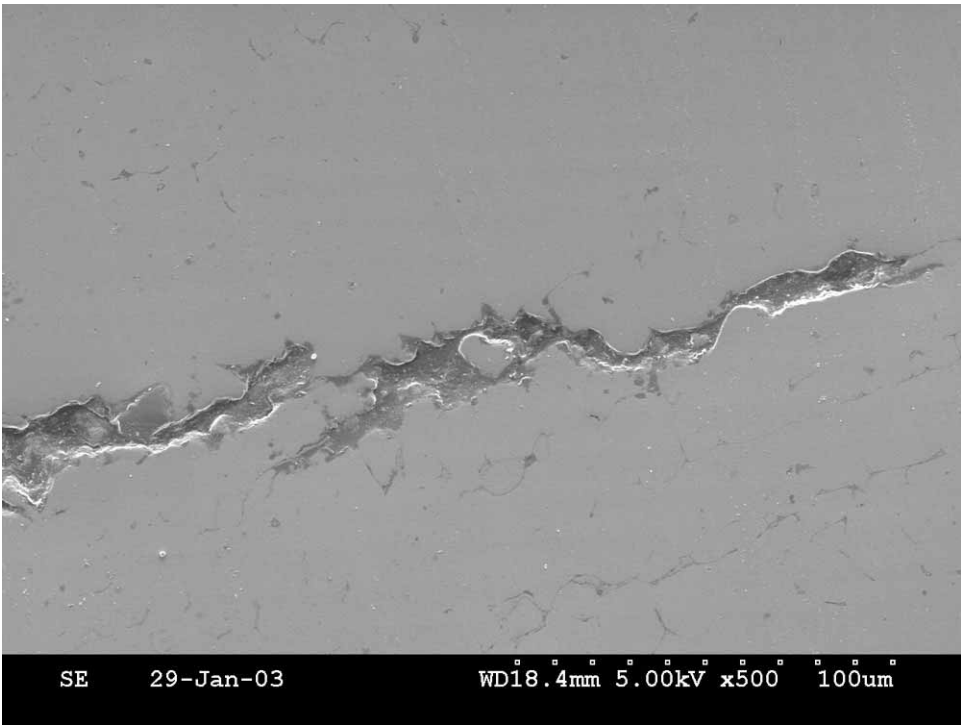
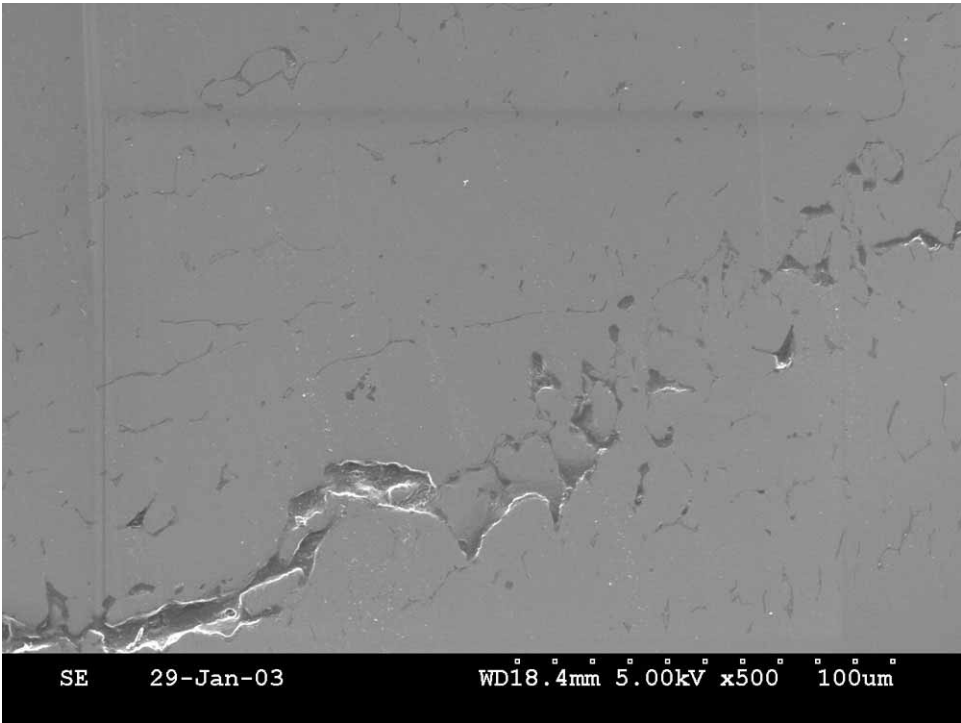


Figure 6.3.2.2: Higher magnification SEM micrographs of crack tip, showing the interdendritic crack path along the elongated ferrite pools.



SE 500X



SE 500X

Figure 6.3.2.3: Secondary electron SEM images of crack tip, showing the interdentritic crack path along the elongated ferrite pools.

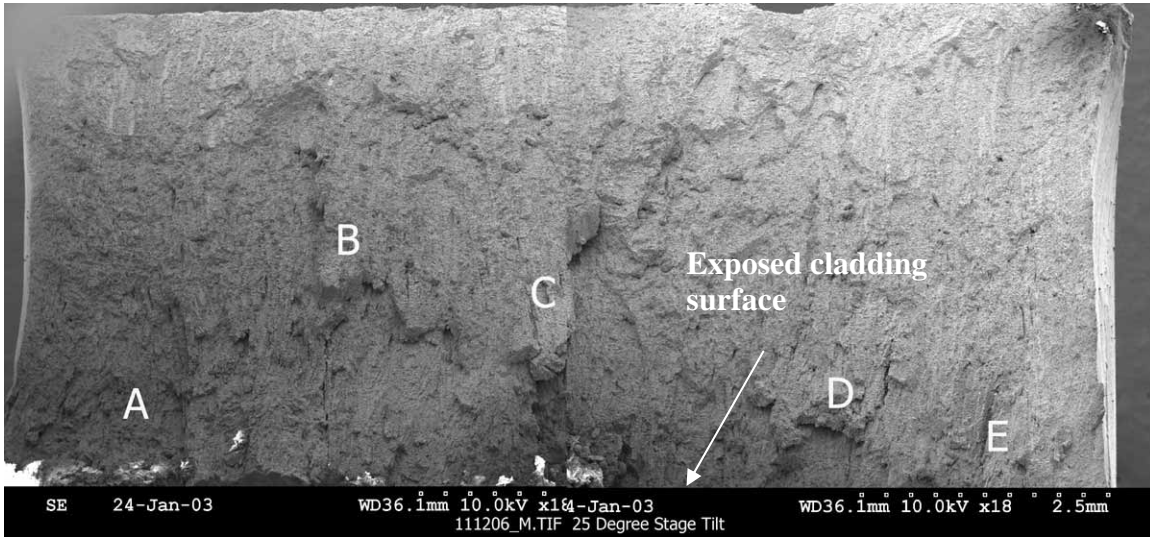
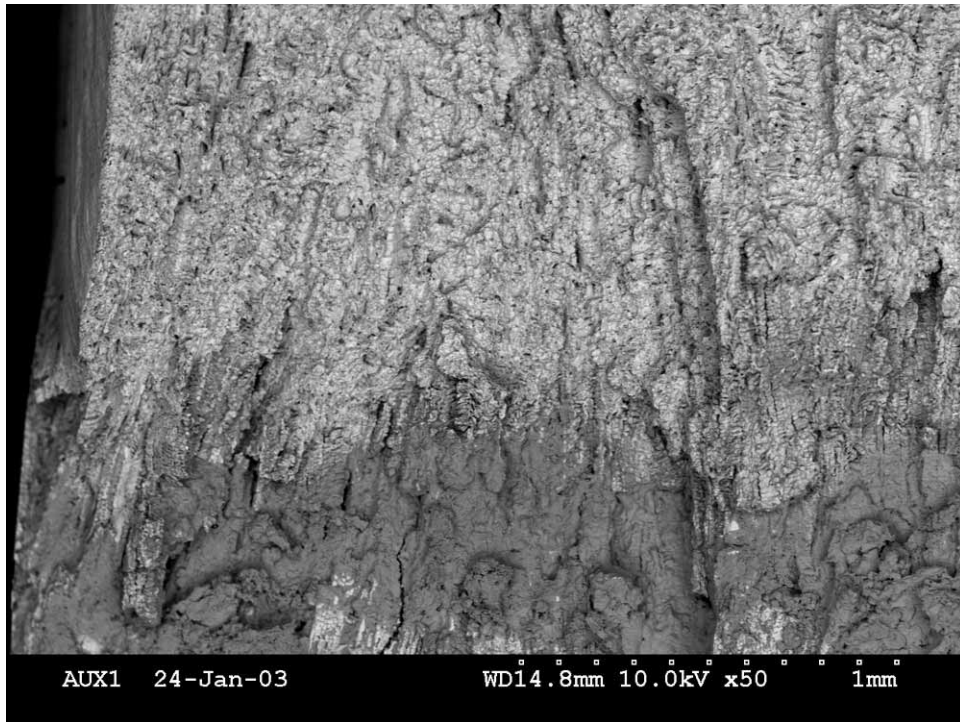
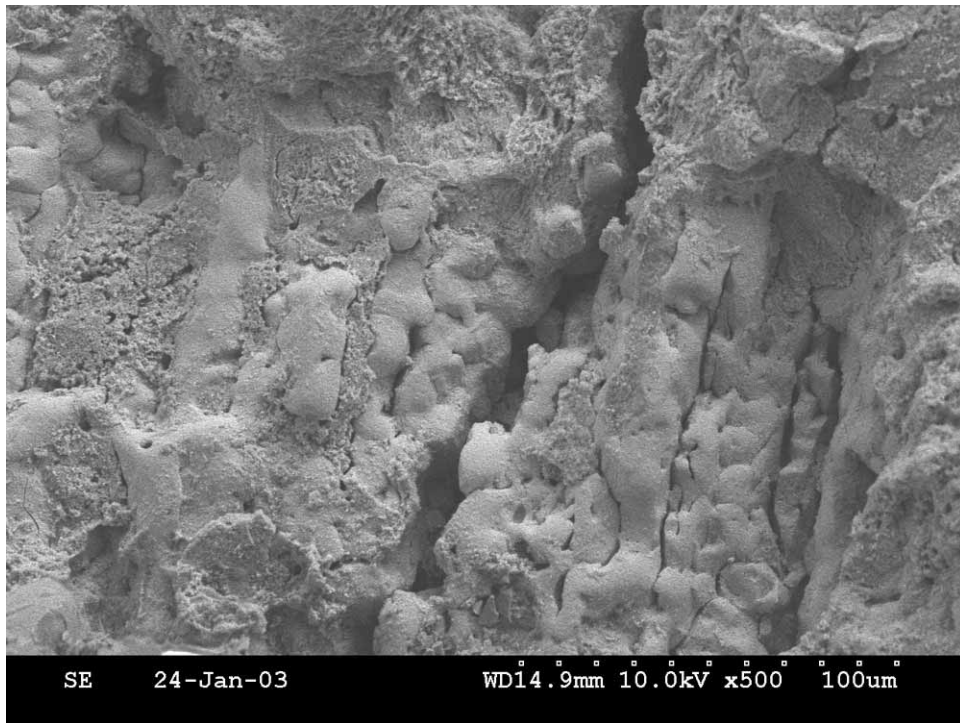


Figure 6.4.1.1: Low magnification SEM mosaic showing the opened main crack (sample A2A7-L1A). Refer to Figures 5.11 and 5.12 for the sample location. The exposed cladding surface is oriented downward in the SEM micrographs.



BSE 50X



BSE 500X

Figure 6.4.1.2: Near mosaic area “A”. Heavy deposits are present toward the exposed side of the cladding (darker contrast in BSE micrograph). Fracture morphology is interdendritic in nature.

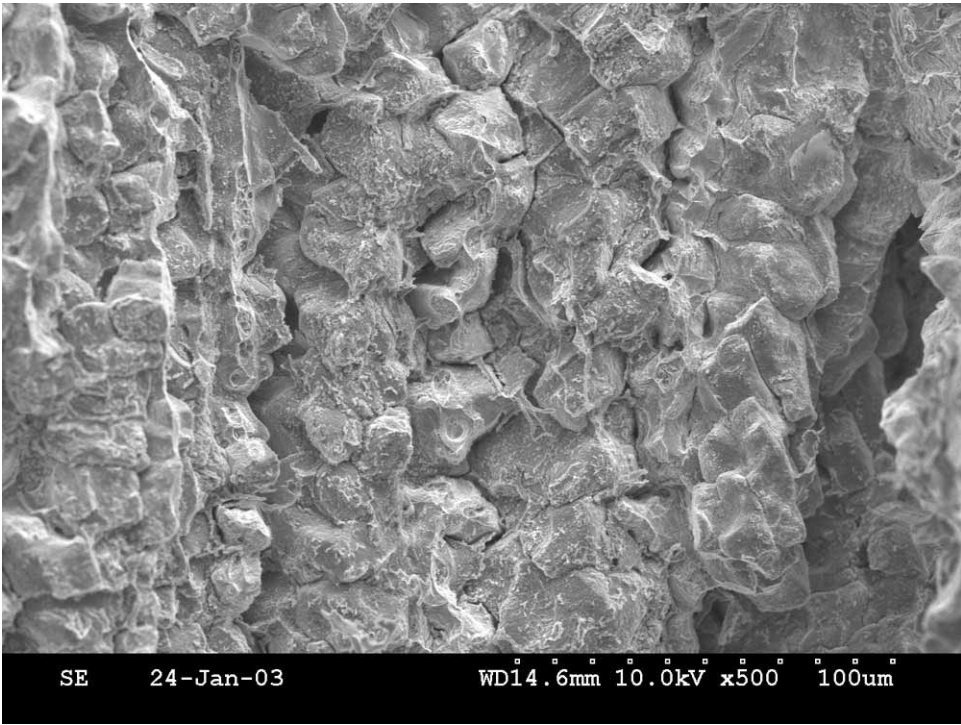
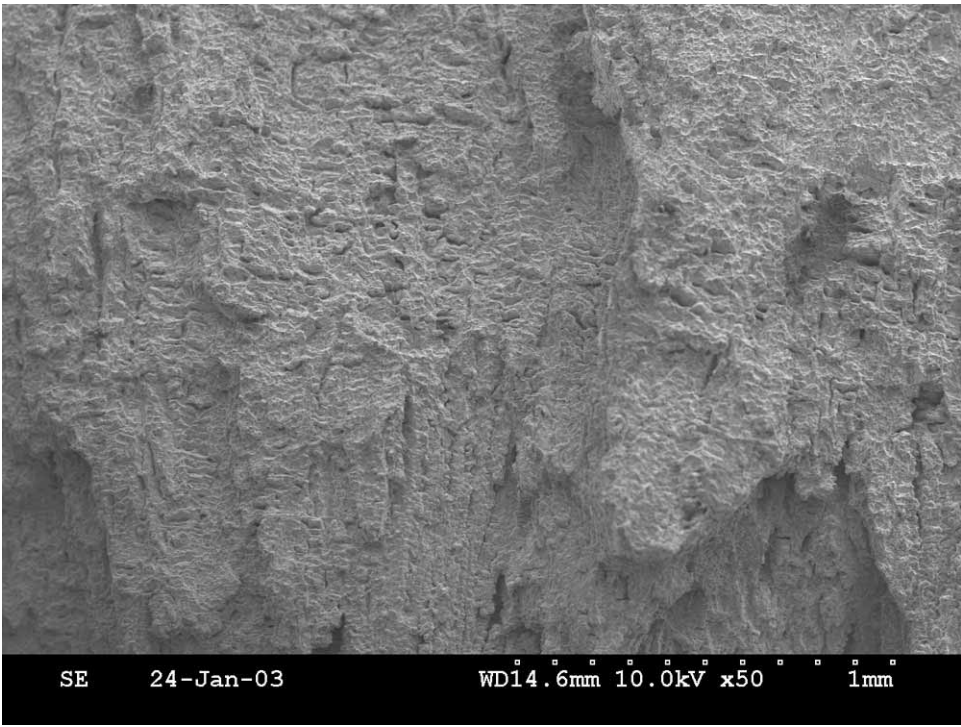


Figure 6.4.1.3: Near mosaic area "B". Cracking is intergranular/interdendritic.

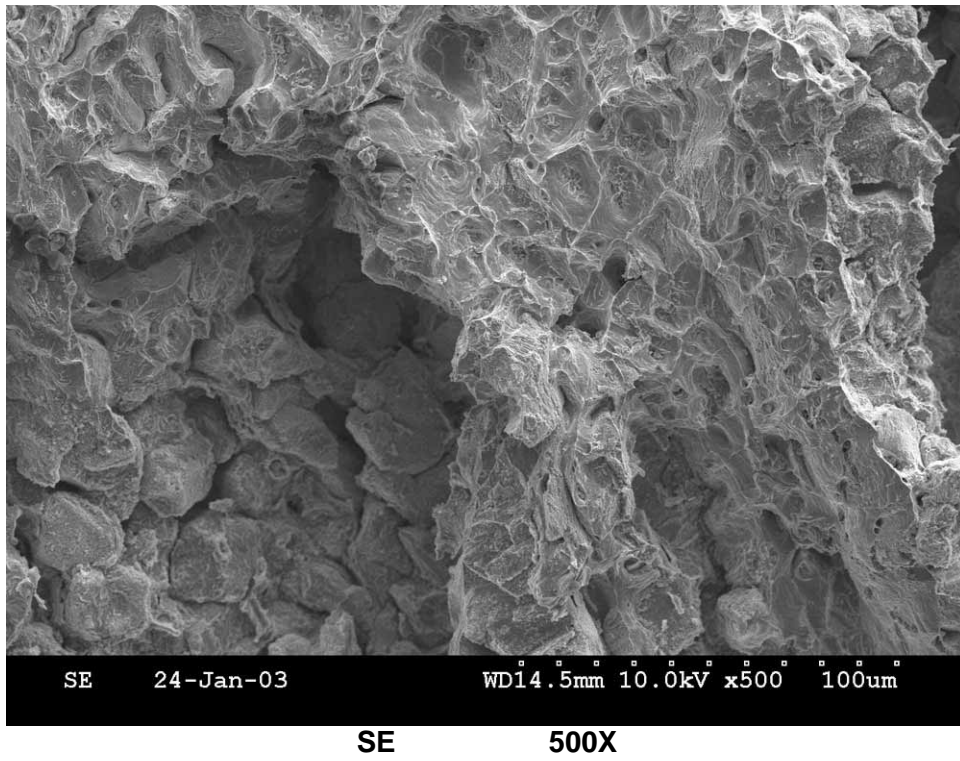
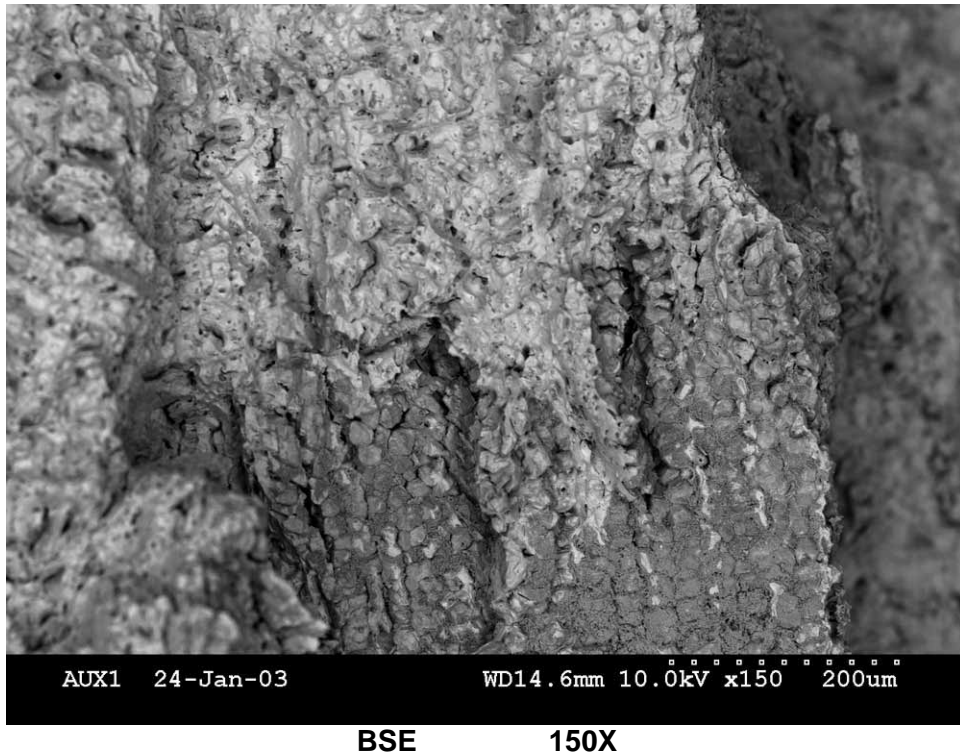


Figure 6.4.1.4: Near mosaic area "C". Fracture mode is intergranular or interdendritic for in-service cracking and ductile tearing for lab opened-up fracture.

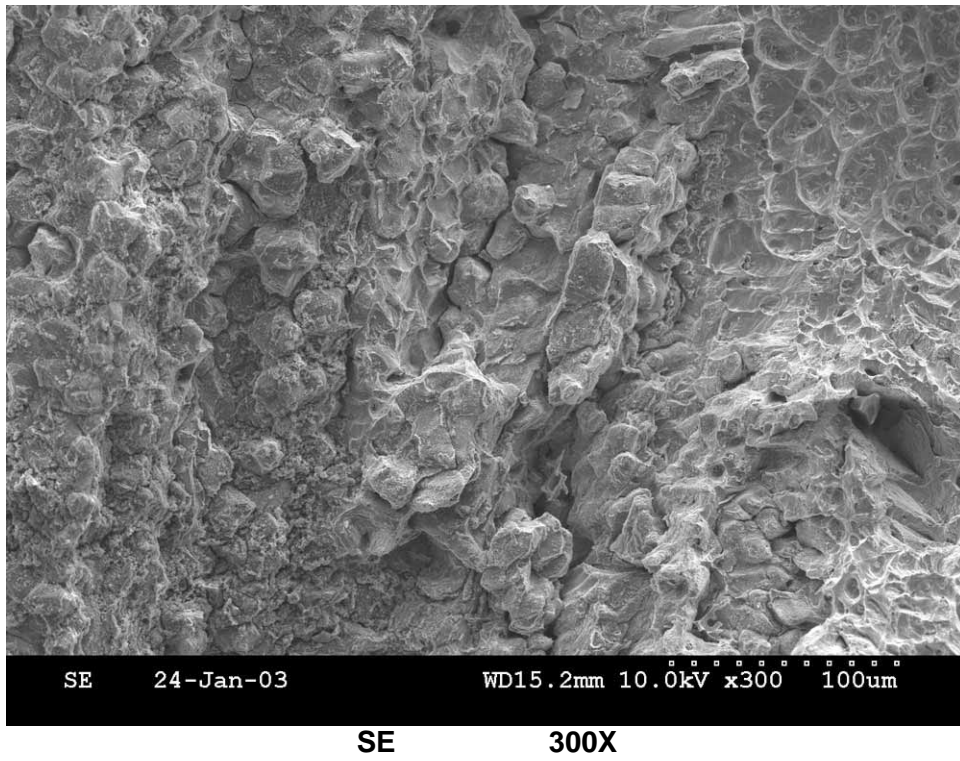
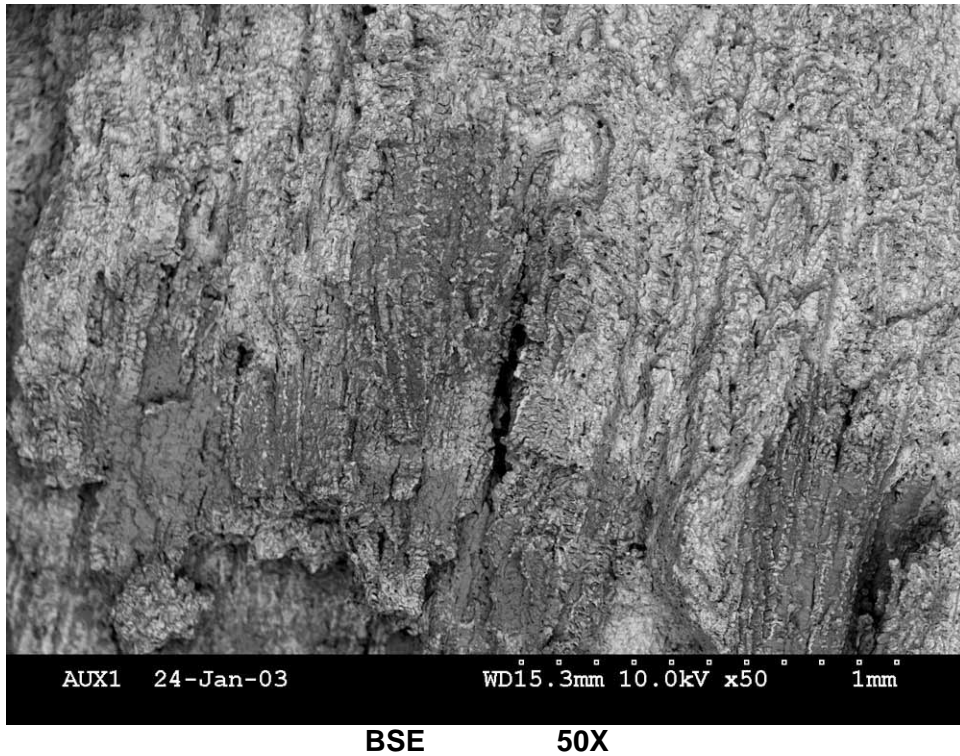
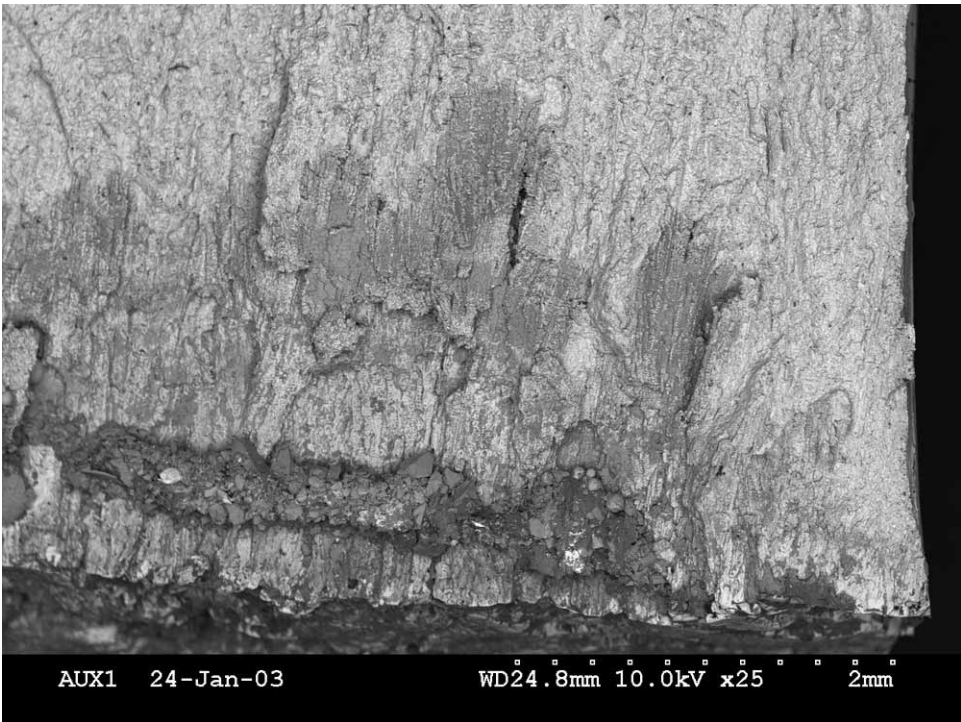
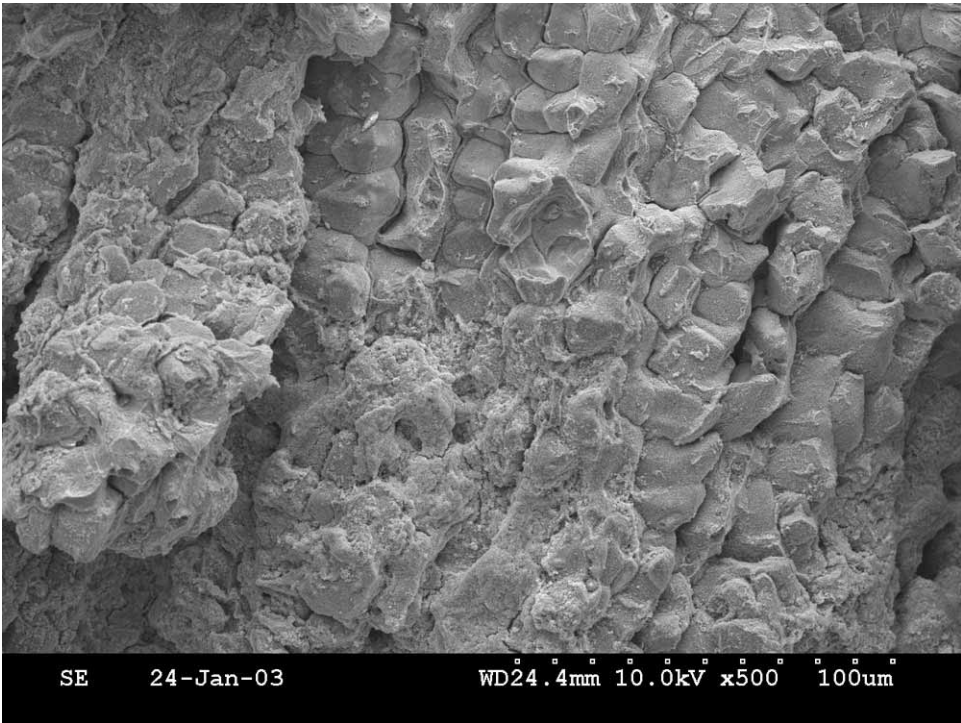


Figure 6.4.1.5: Near mosaic area "D". Fracture mode is intergranular or interdendritic for in-service cracking and ductile tearing for lab opened-up fracture (upper right).

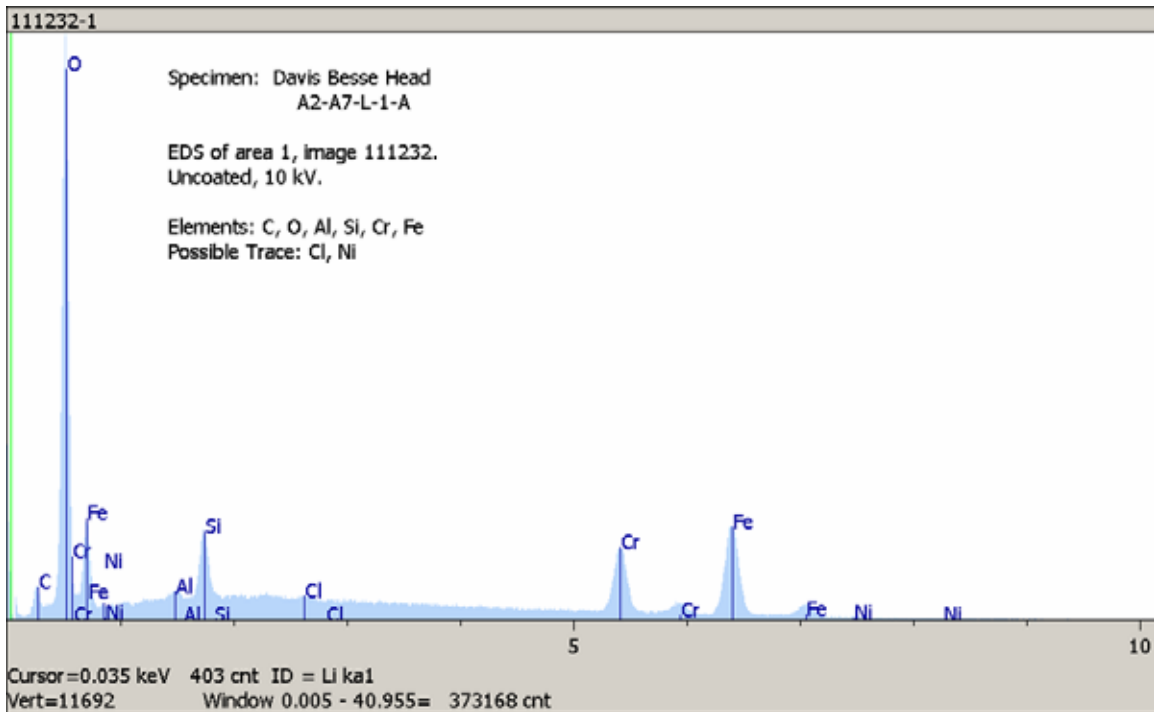
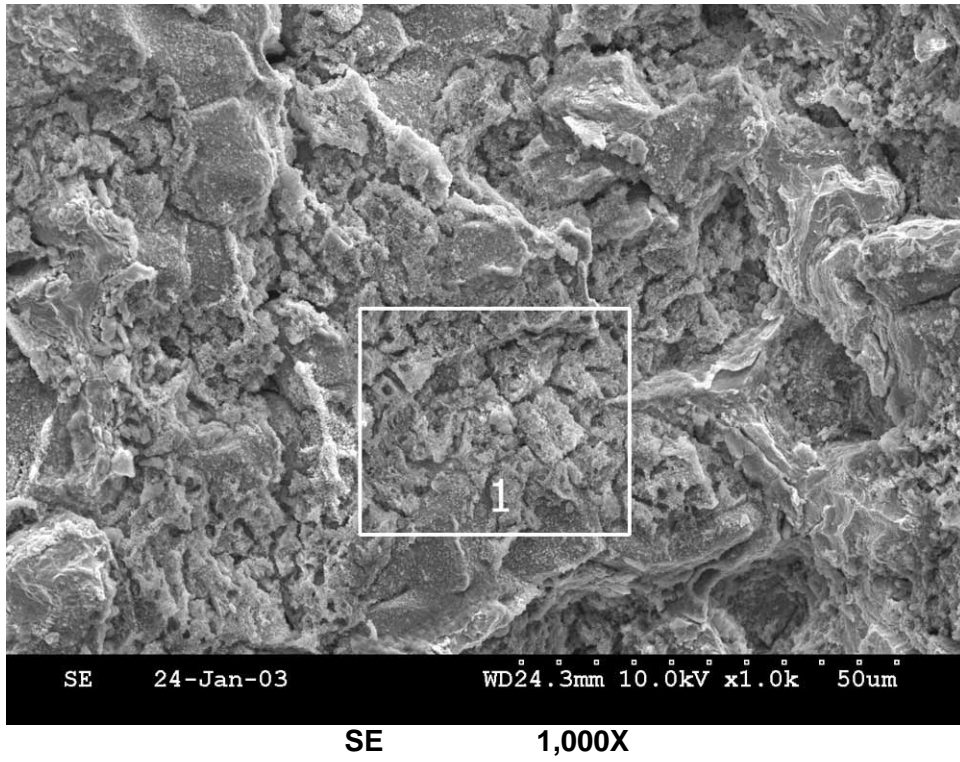


BSE 25X



SE 500X

Figure 6.4.1.6: Near mosaic area "E". Cracking is intergranular/interdendritic.



EDS results for area 1 above.

Figure 6.4.1.7: SEM micrograph and EDS results for deposited region near area "E". The corrosion deposits contained carbon, oxygen, along with iron, aluminum, silicon, and chromium. Possible trace levels of nickel and chlorine were also detected in this area.